The VT1 Shape Memory Alloy Heat Engine Design

by

Jillcha Fekadu Wakjira

Thesis submitted to the Faculty of
the Virginia Polytechnic Institute and State University
in partial fulfillment of the requirements for the degree of

Master of Science

in

Mechanical Engineering

Dr. Charles Reinholtz, Chairman
Dr. Will Saunders
Dr. Don Leo

January 2001
Blacksburg, VA

Keywords: Heat Engine, Shape Memory Alloy, and Intelligent Material

The VT1 Shape Memory Alloy Heat Engine Design

Jillcha Wakjira

(Abstract)

The invention of shape memory alloys spurred a period of intense interest in the area of heat engines in the late 70's and early 80's. It was believed that these engines could use heat from low temperature sources such as solar heated water, geothermal hot water and rejected heat from conventional engines as a significant source of power. The interest has since dwindled, largely because small prototype devices developed in the laboratory could not be scaled up to produce significant power. It is believed that the scaled-up designs failed because they were dependent on friction as the driving mechanism, which led to large energy losses and slip. This thesis proposes a new chain and sprocket driving mechanism that is independent of friction and should therefore allow for large-scale power generation.

This thesis begins by presenting properties and applications of shape memory alloys. The proposed design is then described in detail, followed by a review of the evolution that led to the final design. A brief chapter on thermodynamic modeling and a summary chapter suggesting improvements on the current design follow.

Acknowledgments

Nobody in the Mechanical Engineering department deserves more gratitude than Dr. Charles Reinholtz, who served as the chairman of my thesis committee members and as my advisor for nearly three years, during my stay, here at Virginia Tech. Dr. Reinholtz has been there, for me and other students, through thick and thin. Like a friend you chat with me, like a father you advised me, and like an adviser you corrected me. Thank you, Dr. Reinholtz, for all that you did for me and for the many Mechanical Engineering students that stepped foot in the Randolph building.

Dr. William Saunders, thank you for all the advice you offered me. Thanks for teaching my favorite class, Mechatronics. It is one of the best classes that Virginia Tech is offering. Thanks also for serving in my committee.

I also want to thank Dr. Don Leo for serving in my committee.

Thanks to all the people who helped me complete my project, including Jackie Buhrdorf, for the efficient assistance in the office duties like ordering parts, "Mama Riess" for all the help with the confusing and sometimes frustrating course schedules, Jerry Lucas and Derwin Stafford, for all the help in the machine shop, and Ben Poe for all the computer assistance.

Thanks to my dear friend Colin. Thank you for being there for me. May God help me not to forget your kindness and friendship. Thanks for teaching me Mechanical Desktop; it is one great program, and thanks for all the water you brought me all the way from your home in Roanoke.

To my family, my father, Fekadu, my mother Abinet, and my sisters Nassissie and Lemene, thanks for helping me get where I am. Thanks for the confidence you had in me and the encouragement you gave me since childhood.

To my fiancee, Sidu, thanks for the encouragement you offered me during the course of this project. Your sincere advice and comments, your courage and strength had a valuable role in this project, my education, and our relationship. I love you. May God bless our marriage.

I want to conclude by thanking God, for supporting me throughout this project. He has been the source of my strength and courage; the source of my hope and vision. Thank you for all that you did in my life, especially for sending your son, Jesus Christ, to save me. Praise and honor be to you!

Contents

List of Figures ----------VII

Chapter 1: Introduction

Motivation ---------- 2

History of SMA Heat Engines ---------- 3

The VT1 SMA Heat Engine ---------- 4

Chapter 2: Shape Memory Alloy Properties and their Applications

Introduction---------- 6

Metallurgical Property of NiTi Alloy ---------- 7

The Shape Memory Phenomenon ---------- 7

Effect of Composition, Annealing, and Stress on the Transition

Temperature of SMAs ---------- 15

Typical Mechanical Behavior of Nitinol Alloys ---------- 17

Applications of Shape Memory Alloys ---------- 21

Couplings ---------- 22

Biomedical and Medical Applications ---------- 23

Actuators ---------- 26

Heat Engines ---------- 29

Other Applications ---------- 29

Chapter 3: Early Works

Introduction ---------- 31

Heat Engine by Ridgway Banks [US3913326] ---------- 31

Heat Engine by Alfred Davis Johnson [US4055955, 1977] ---------- 35

Heat Engine by John J. Pachter [US1975000732471]---------- 37

Chapter 5: Design of the VT1 SMA Heat Engine

Introduction ---------- 39

The Assembly ---------- 40

The SMA Chain ---------- 42

The Roller Chain Assembly ---------- 43

The Pin ---------- 44

The SMA Wire ---------- 45

The Sprockets ---------- 50

Synchronizing Chain ---------- 53

Straining The SMA Chain ---------- 53

Chapter 5: Progressive Design of the VT1 SMA Heat Engine

Introduction ---------- 57

Pulley-Type Design ---------- 59

Static Model ---------- 59

Dynamic Model ---------- 62

Design I: The engine without a synchronizer ---------- 63

Design II: An engine with a timing belt synchronizer ---------- 64
Design III: An engine with a roller chain synchronizer ---------- 64
Design IV: Sprockets with Different Pitch, but with the Same Number of Teeth 67

Chapter 6: Thermodynamic Modeling of the VT1 SMA Heat Engine

Introduction ---------- 70
Carnot Engine for a Liquid-Gas System ---------- 71
SMA Heat Engine Limitation ---------- 75
Limitations on the Performance of the Engine ---------- 81

Chapter 7: Conclusions and Recommendations ---------- 83

Appendix A: Reference

Books ---------- 85
Patents ---------- 87
Web Page ---------- 88

Appendix B: Parts List and Drawings of Parts that were Manufactured in House

Drawings

8-32 Bolt ---------- 90
Bolt Assembly Exploded View ---------- 91
Frame 1 ---------- 92
Frame 2 ---------- 93
Shaft ---------- 94
Bearing Spacer ---------- 95
Sketch of a 0.78" Pitch Sprocket ---------- 96

Vita ---------- 97

List of Figures

Figure 2.1: Nickel-Titanium phase diagram ---------- 8

Figure 2.2 (a) and (b): The Crystalline Structure of Martensite and Austenite Phase ---------- 9

Figure 2.3: The Shape Memory Effect Process ---------- 11

Figure 2.4: Typical transformation strain versus temperature curve ----------13

Figure 2.5: Optical micrographs of the growth of a SMA crystal due to cooling ------- 14

Figure 2.6: Variation of A_s with Nickel Content (Buehler, 1967) ---------- 16

Figure 2.7: Martensite stress-strain behavior at temperatures below the martensite finish temperature ---------- 18

Figure 2.8: Austenite Stress-Strain Behavior at temperatures above the austenite finish Temperature ----------18

Figure 2.9: Stress-Strain Plot for comparison of the Austenite and Martensite level of stress ---------- 20

Figure 2.10:Shape Memory Alloy Pipe Coupling ---------- 23

Figure 2.11: Nitinol wire used in a band for connecting bones ---------- 25

Figure 2.12: TiNi Filter inserted into the vena cava of a dog ---------- 26

Figure 2.13: Schematic diagram of a simple two-way actuator using a dead weight bias ---------- 27

Figure 2.14: The Mars Pathfinder used a Nitinol actuation for the first time outside the earth's atmosphere ---------- 28

Figure3.1: The inventor Ridgway Banks and machinist Hap Hagopian working on a prototype of the first SMA heat engine ---------- 32

Figure 3.2: A plan view of Banks' heat engine ---------- 33

Figure 3.3: (a) Johnson's engine using nitinol in the form of a continuous helix, synchronized using gears. **(b)** A modified form of engine **(a)** ---------- 35

Figure 3.4: A simplified representation of Pachter's engine ---------- 37

Figure 4.1: 3D Representation of the VT1 heat engine assembly ---------- 40
Figure 4.2: 3D CAD drawing of the SMA roller chain assembly ---------- 43
Figure 4.3: AutoCAD drawing of the fixture that holds the aluminum screw in place during machining---------- 45
Figure 4.4: Sketch for computation of chain length ---------- 47
Figure 4.5: Standard sprocket tooth form for roller chains ---------- 51
Figure 4.6: Sketch for demonstrating method of straining ---------- 54
Figure 4.7: Sketch of sprocket showing the four wires that are part of the SMA Chain ---------- 55

Figure 5.1: Sketch of the VT1 Nitinol Heat Engine that uses pulley-type design ------- 59
Figure 5.2: **(a)** Free body diagram of pulley-1 **(b):** Free body diagram of pulley 2 ----- 60
Figure 5.3: (a) Free body diagram of pulley-1 **(b):** Free body diagram of pulley 2 ----- 62
Figure 5.4: Sketch of a sprocket /chain system ---------- 65
Figure 5.9: Sketch showing four sprockets with teeth numbers N_1, N_2, N_3, and N_4. ---- 66

Figure 6.1: Steady-flow Carnot engine using a liquid-vapor mixture as working substance ---------- 72
Figure 6.2: Sketch of Pressure-volume relationship of a liquid-gas system ---------- 73
Figure 6.3: Plot of stress- strain relationship for a 0.5mm nitinol wire held at a series of fixed temperatures. ---------- 76
Figure 6.4: Theoretical plot of temperature versus entropy of a heat engine ---------- 78
Figure 6.5: Sketch of the VT1 Nitinol Heat Engine ---------- 80

Chapter 1

Introduction

Concern for the well-being of our planet and mankind's ever expanding need for power has generated considerable interest in alternative ways of generating power. Many different methods of producing power, such as fuel cells and solar panels, have been developed and refined in recent years. The Nitinol heat engine, discussed in this thesis, is also a result of this growing interest in the quest for alternative power sources.

Nitinol, an alloy of Nickel and Titanium, is a material that possesses unique physical and metallurgical properties. It can be made to memorize some previously defined shape. The material can then be deformed plastically, and when is subjected to appropriate thermal conditions, it will return to the memorized shape. This shape change comes about as a result of the material changing phase while still a solid.

Numerous inventors have used this special property to develop designs that are finding a range of applications in the commercial world. For example, over one hundred thousand (100,000) shape memory alloy couplings have been installed in the hydraulic systems of the famous F-14 jet fighter. The Material Adhesion Experiment (MAE) aboard the Mars Pathfinder/ Sojourner rover has demonstrated the first use beyond Earth's orbit of a repeatedly activated device driven by a Shape Memory Alloy. SMAs

(Shape Memory Alloys) are gaining popularity in different sectors of industry including automotive, medical, electronic, and consumer appliance to name a few.

Motivation

A significant amount of energy is not utilized in our ecosystem, as well as in industry. Potential sources of energy include industrial waste heat, geothermal heat, oceanic thermal gradients, and solar radiation. It is a great asset to be able to convert such low-grade energy sources to mechanical work. The major drawback to the exploitation of these sorts of energy sources is the relatively small temperature gradients. Past efforts to generate useful forms of power from small temperature difference heat sources were unsuccessful, because standard recovery techniques generally have not approached competitive efficiency.

The energy crisis in the early 70's and the subsequent petroleum price increase stimulated searches for alternative and previously undeveloped energy sources. The invention presented here relates to an energy conversion system, which effectively uses a temperature differential to convert heat energy to mechanical work. In other words, a heat engine. Unlike conventional heat engines such as gasoline or other fuel type engines, Nitinol heat engines do not require high combustion temperatures.

Most existing heat engines use methods of actuation that are subject to significant frictional losses. Unlike other heat engines, the VT1 heat engine induces actuation using a chain made from a shape memory alloy. Previous attempts to develop SMA heat engines used wire that ran directly on pulleys. Some of the previous inventions and the current state-of-the-art of SMA applications follow in the next couple of chapters.

It is the intention of this thesis to present a heat engine that uses an SMA chain and sprocket design. The engine will continuously convert heat energy directly to useful

mechanical power. The proposed design promises to have improved efficiency compared to previous Nitinol heat engines.

There are a number of advantages to this design. The design uses few parts, which make it inexpensive and easily maintained. It can find application in various environmental conditions, because SMAs are resistant to corrosion. They can withstand salty sea water, industrial effluent, or geothermal brine. In addition, the SMA heat engine can operate over a wide range of temperatures, by selecting a thermal memory material having a suitable critical temperature appropriate to the climatic conditions.

History of SMA Heat Engines

The discovery of shape-memory effect in certain alloys dates back to 1932, when a Swedish researcher named Arne Olader first observed the property in gold-cadmium alloys. The material, when plastically deformed while cool, returned to its undeformed shape when warmed. Several SMA alloys have since been discovered. Some of these alloys include CuSn, InTi, TiNi, and MnCu (Funakubo, 7).

The alloys of TiNi, better known as Nitinol, and the copper-based alloys are the most commonly used, because they can recover substantial amounts of strain, or generate significant force upon changing shape. Besides Nitinol, Flexinol is another kind of shape memory alloy that is becoming popular in industry. Flexinol, like Nitinol, is a shape memory wire. The only difference is that Flexinol has a better actuation property along the line of deformation compared to Nitinol and other SMA materials.

William Bueher, David Goldstein and others developed Nitinol at the Naval Ordinance Laboratory in 1962. The name, "Nitinol," itself derives from the names of the composite elements and the place of discovery; **NI**ckel **TI**tanium **N**aval **O**rdinance **L**aboratory. They noticed that Nitinol, when struck, produced sound that changed with

temperature. Further study revealed the phase change and the associated shape-memory phenomenon (Johnson A.D.).

One of the first applications of SMAs, in the 1970s, was in heat engines. A heat engine is a mechanism that is capable of converting heat energy to mechanical or electrical energy. The idea developed from a rubber band heat engine that was in existence long before SMAs were discovered. The discovery of SMAs made it easy to do the energy conversion at typical water temperatures, which is a desirable feature when we think of its application in extracting energy from the sea.

Chapter 3 will present a few of the many heat engine inventions that are on file in the U.S. patent office. Some of the early inventors include William J. Buehler (Buehler,1968), Paul F. Horton (Horton, 1977), Sandoval J. Dante (Dante, (1977), Alfred Davis Johnson (Johnson, 1977), Peter A. Hochstein (Hochstein, 1977), Warren K. Smith (Warren, 1978), Yao Tzu Li (Li, 1978), and John J. Pachter (Pachter, 1979),

Most of the previous SMA heat engine work involved SMA wire or a coil and a series of pulleys. In the process of conversion, significant energy is lost as friction work between the pulleys and the wire. To be practical, these engines would typically be required to deliver hundreds of kilowatts, and this proved to be much more difficult than anticipated. For all of these devices scale-up stopped at about one kilowatt. In other words, the inventions failed for engineering and economic reasons (http://www.sma-mems.com/act98.htm). This thesis tries to tackle the problem of scale-up by proposing a new kind of heat engine, which we will call the VT1 heat engine.

The VT1 SMA Heat Engine

The work presented, in this paper, reports that losses such as friction can be minimized by using SMA chains that engage into a sprocket, instead of a pulley-wire or pulley-coil actuation. The VT1 heat engine uses an improved alloy called Flexinol,

which shows improved shape memory effect, compared to regular Nitinol alloys. Currently, the engine is still under construction, but I will present the progressive design of the engine and the details of the final design. Appendix B presents the technical drawings of the parts that were built in house and those that are yet to be manufactured. Parts that were purchased are also listed in this Appendix.

Chapter 2

Shape Memory Alloy Properties and their Applications

Introduction

In this chapter, we will review the properties that are characteristic of shape memory alloys (SMAs). We begin by looking at the metallurgical properties from microscopic level, and move on to explain how the phase changes that we observe microscopically bring about the shape memory effect that we physically observe. We then explain the typical parameters that affect the physical performance of the alloy, such as stress, strain, and annealing.

Two main characteristics identify shape memory alloys (SMAs), shape memory effect and pseudoelasticity. By training the SMAs at a given temperature, they can be made to memorize a specific configuration, which can be activated via temperature change or via externally applied load. They can sustain a large amount of strain, suffer no permanent plastic deformation, and recover their original length upon heating.

Metallurgical Property of NiTi Alloy

Unlike other metallic materials, SMAs undergo large amount of deformation without permanent deformation. Not only can they sustain large deformations, they can recover that strain upon temperature change or /and loading. This characteristic of SMAs is due to their unique phase transformation mechanism. One type of SMA is Nitinol, which we will use as an example in explaining the unique characteristic of SMAs.

The Shape Memory Phenomenon

A reversible, solid phase transformation known as martensitic transformation is the driving force behind shape memory alloys. When nickel and titanium atoms are present in the alloy, in a given proportion, the material forms a crystal structure, which is capable of undergoing a change from one form of crystal structure to another. Temperature change or/and loading initiate this transformation

In 1965, a patent was given to metallurgists Buehler and Wiley for their development of the NiTi alloy series; 55-Nitinol was the name given to the alloy. The 55 refers to the nickel percentage composition in the alloy (Dye, 5). Typical Nickel-Titanium alloy contains 49 to 57 percent Nickel. The composition of Nitinol, as illustrated on the nickel-titanium phase diagram in Figure 2.1, has a titanium composition varying from 0 to 50%, but the ideal composition of Nitinol can only vary between 38% and 50% titanium by weight. Only this composition of Nitinol possesses the shape-memory characteristics.

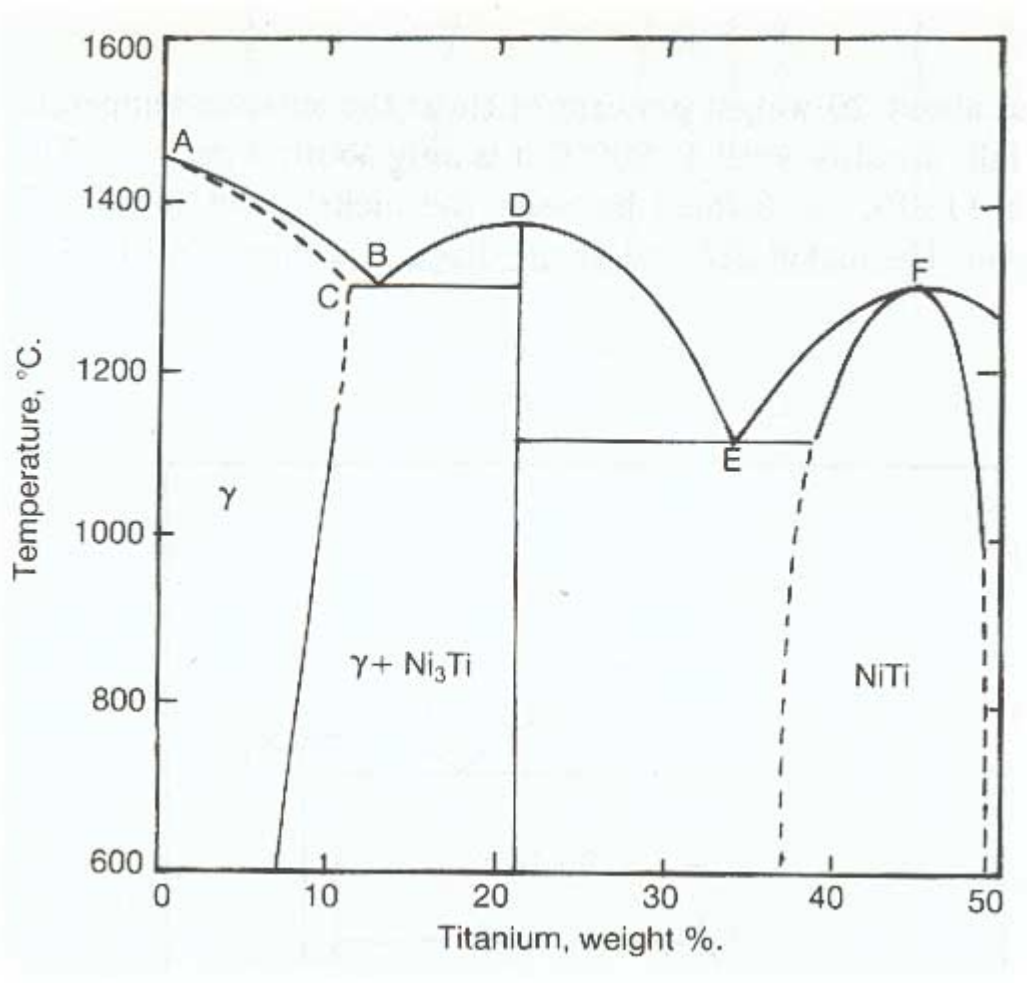

Figure 2.1: Nickel-Titanium phase diagram [Betteridge, 52]

The transition from one form of crystalline structure to another creates the mechanism by which the shape change occurs in SMAs. This change involves transition from a monoclinic crystal form (martensite) to an ordered cubic crystal form (austenite). The austenite phase is stable at high temperature, and the martensite is stable at lower temperatures. Figure 2.2a and 2.2b are two-dimensional representations of the austenite and martensite crystal structures.

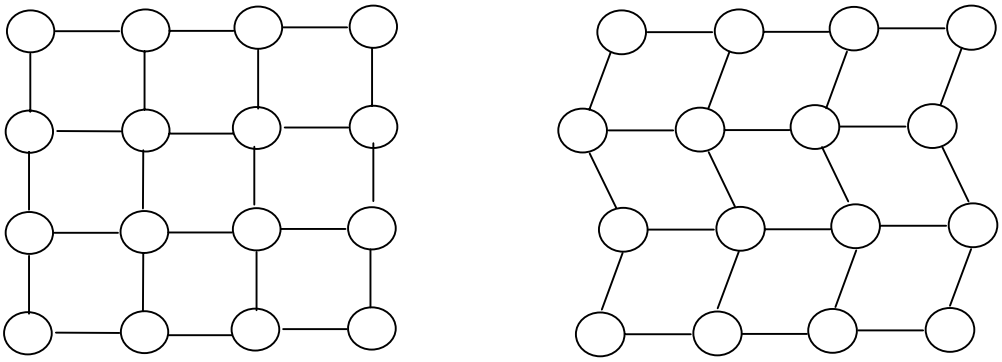

(a): High temperature austenite cubic structure

(b): Low temperature martensite (twinned) lattice structure

Figure 2.2 (a) and (b): The Crystalline Structure of Martensite and Austenite Phase [Hodgson, 1988]

In the martensite phase, atoms orient themselves in rows that are tilted left or right. We refer to this phenomenon as twinning, because the atoms form mirror images of themselves or twins. The martensite twins are able to flip their orientation, in a simple shearing motion, to the opposite tilt, creating a cooperative movement of the individual twins. This results in a large overall deformation.

Heating a deformed SMA causes the atoms to reorient themselves in such a way that the martensite lattice starts to untilt. Consequently, the original shape of the piece forms. Figure 2.3 shows this shape memory process.

In ordinary metals, deformation occurs by dislocation motion and atomic planes sliding over one another, taking on a new crystal position. Increased tangles of dislocations will not allow the metals to reverse the deformation, thus resulting in permanent damage to the crystalline order. Unlike regular metals, SMAs deform by

detwinning (changing the tilt of a twin orientation), which does not cause any dislocation. Detwinning is a shearing motion that allows the martensite phase to absorb dislocation, to a given extent. For complete shape recovery to occur, the deformation process should not involve slip, because slip is an irreversible process.

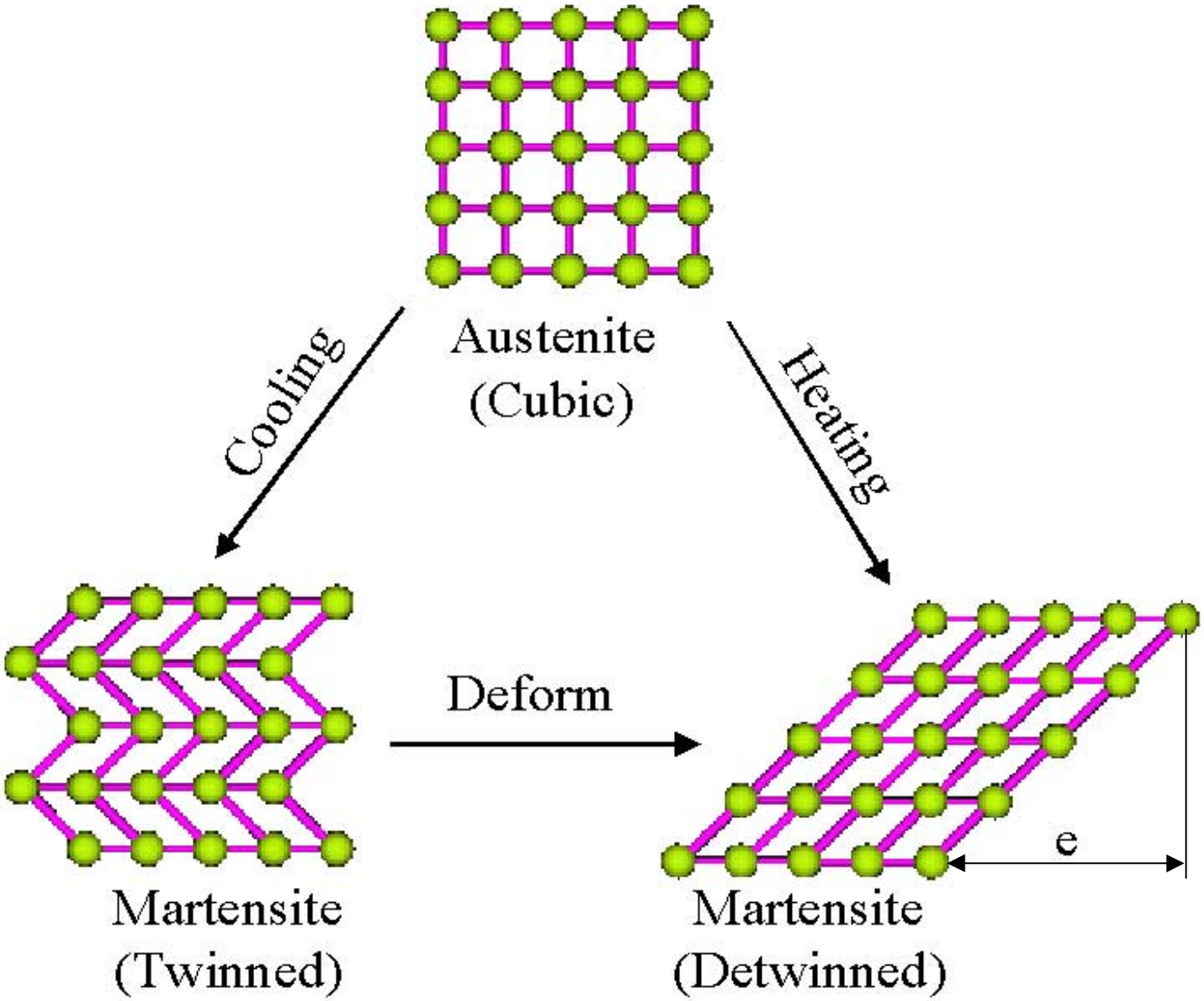

Figure 2.3: The Shape Memory Effect Process [Hodgson, 1988]

When a SMA is in its austenite phase, it exhibits a highly elastic behavior. This allows the material to deform up to 7% and then fully recover the resulting strain by simply removing the load. This behavior is known as the pseudoelastic effect or pseudoelasticity; some people refer to pseudoelasticity as superelasticity. Deforming a pseudoelastic material results in the formation of a martensite crystal. The martensite formed in this forward transformation is called stress-induced martensite (Dye, 8).

Even though pseudoelasticity is an important characteristics of SMAs, typical applications of these materials require use of the shape memory effect, which is a result of temperature induced transformation. The value of this transformation temperature depends on the composition of the alloy. In fact, this temperature is adjustable, from over 100^{o}C down to cryogenic temperatures (Technical Characteristics of Flexinol actuator wires, Dynalloy, Inc.). The following section presents the effect of temperature and stress on the transition

The temperature-induced transformation of SMAs occurs in three stages, which I will designate as stage (I), stage (II) and stage (III). Heating a shape memory alloy specimen triggers transformation of the low-temperature phase (III) to the intermediate phase (II), then to the high-temperature phase (I). As it is demonstrated in figure 2.4, the "transformation temperature" does not exist at a single temperature, but a rage of temperatures, which are called characteristic temperatures.

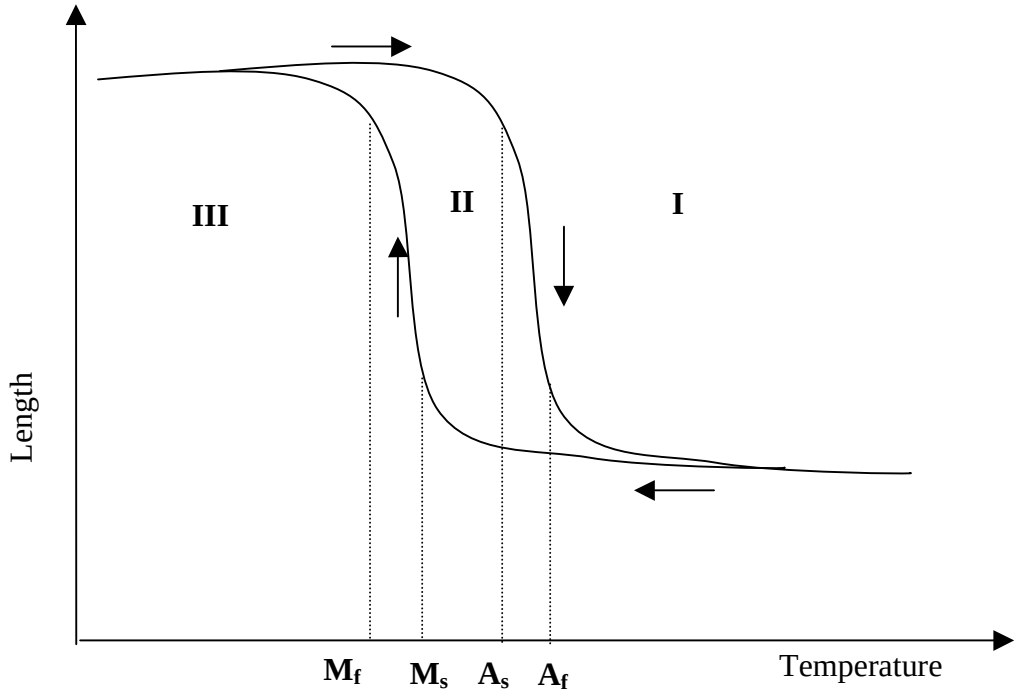

Figure 2.4: Typical transformation strain versus temperature curve
M_f, M_s, A_s, and A_s are martensite finish, martensite start, austenite start, and austenite start temperatures respectively.
[http://www.sma-inc.com/SMAPaper.html, 2]

The first characteristic temperature is the martensite start temperature (M_s). The martensite phase starts forming above this temperature. Study shows that martensite typically occurs as alternately sheared platelets, which are seen as herringbone structure when viewed metallographically (Figure 2.5). The figure shows an interesting view of a crystal that is undergoing physical change in the microscopic level.

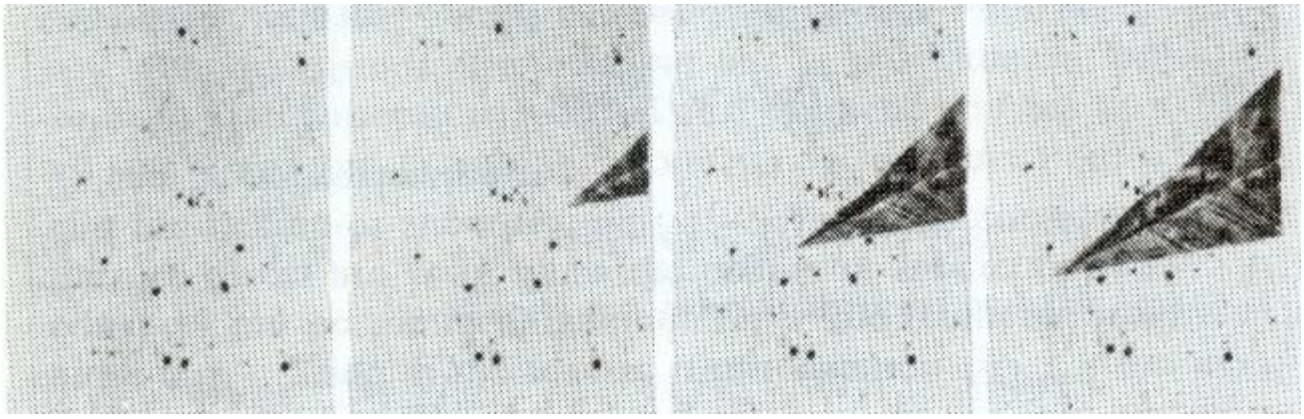

Figure 2.5: Optical micrographs of the growth of a SMA crystal due to cooling [Funakubo, 9]

Martensitic transformation results from a lattice transformation, wholly, without atomic diffusion, which means that the concentration of solute atoms dissolved in the martensite phase is equal to that in the parent (initial) phase. The transformation involves shearing that results from cooperative atomic movement. The transformation terminates at temperature close to, M_f, as the temperature decreases.

The next set of characteristic transformation temperature is the austenite start and finish temperature, A_s and A_f respectively. The austenite phase starts forming as a SMA is heated at about A_s. A rigid, tough, face-centered cubic crystal structure starts forming, and the transformation is complete at temperature, A_f. When a SMA specimen is heated beyond A_f, it will result in a complete recovery of the strain; this is the shape memory effect. A complete shape recovery is said to occur when a SMA returns to a parent phase that is identical to the initial phase.

Effect of Composition, Annealing, and Stress on the Transition Temperature of SMAs

The primary method of changing the transformation temperature of a SMA is by changing the composition of the alloy. Figure 2.6 shows a plot of the variation in austenite start temperature with respect to the composition of Nickel. SMA's can now be engineered to have a transition temperature that is within two degrees of the desired temperature.

The other factor that affects transition temperature is the state of stress. The transition temperature increases with stress (Duval, et. al.). If a SMA is stressed to the point that a deformed martensite forms, then the A_s occurs at a higher temperature. This is because overcoming the increased stress requires additional heating energy.

Annealing is a process where by the metal is constrained in a given shape and heated to the annealing temperature. A SMA is made to remember its shape by using an annealing process. SMAs can be annealed between 450 and 800 ^{o}C. Besides annealing, processes such as cold swaging and drawing cause residual stresses to occur locally within the material's microstructure (Goldstein et al 1987). These stresses will significantly increase the transformation start and finish temperatures.

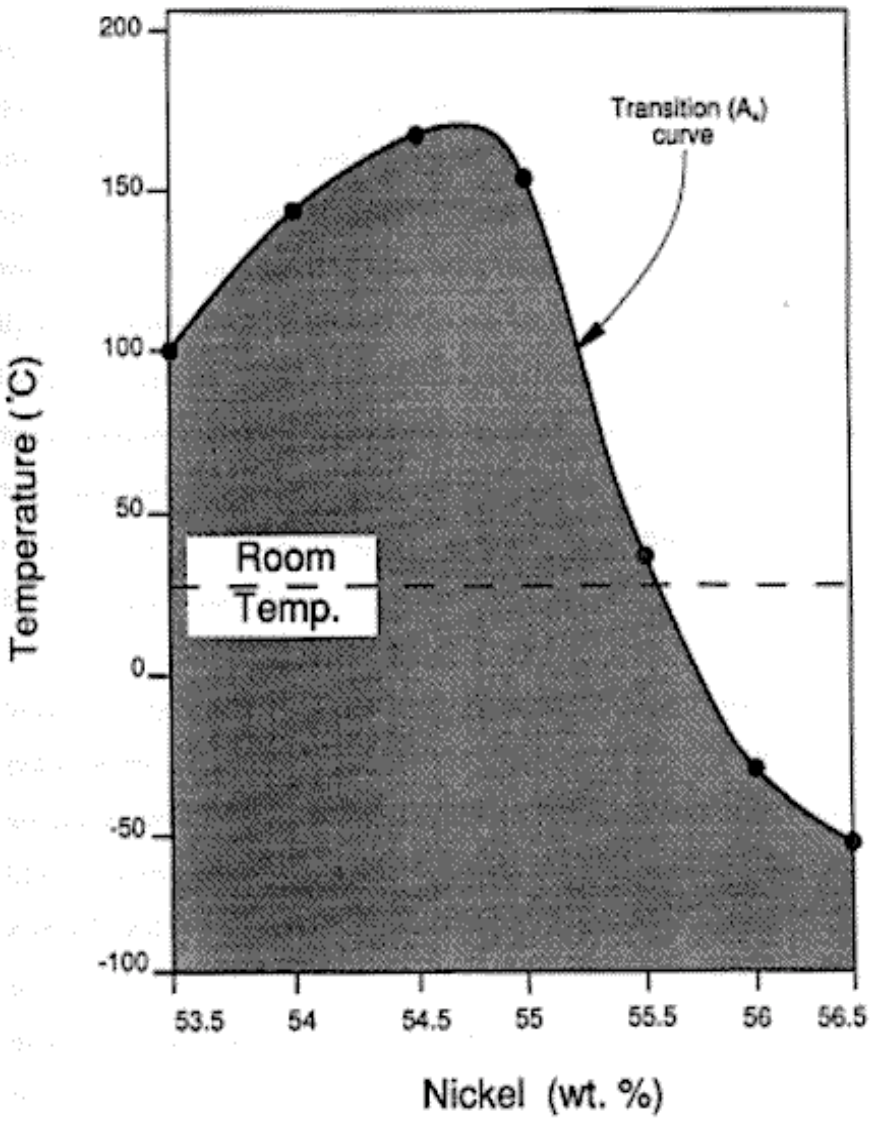

Figure 2.6: Variation of A_s with Nickel Content (Buehler, 1967)

When enough energy is supplied to the material in the form of temperature gradient or stress, some phase transformation occurs.

There is one important point to make note of before moving to the next section. Notice in Figure 2.4 that the path taken during heating is not the same as the path taken, during cooling; hysteresis is present in SMAs. Internal friction caused by the movement of the austenite-martensite interface causes the presence of hysteresis. The width of the hysteresis loop depends on the alloy composition and processing. Like the transition temperature, the hysteresis width can be contained within few degrees by precisely engineering the contents of the alloy.

Typical Mechanical Behavior of Nitinol Alloys

This section is an extension of the discussion above. It provides a brief discussion of stress-strain behavior of SMAs. We will first look at the stress-strain behavior of the martensite phase.

Figure 2.7 shows the stress-strain behavior of a SMA in its martensite state. Figure 2.8 shows the behavior when the SMA is in its austenite phase. Although the shapes of the curves are similar, the scale of the two figures are not the same.

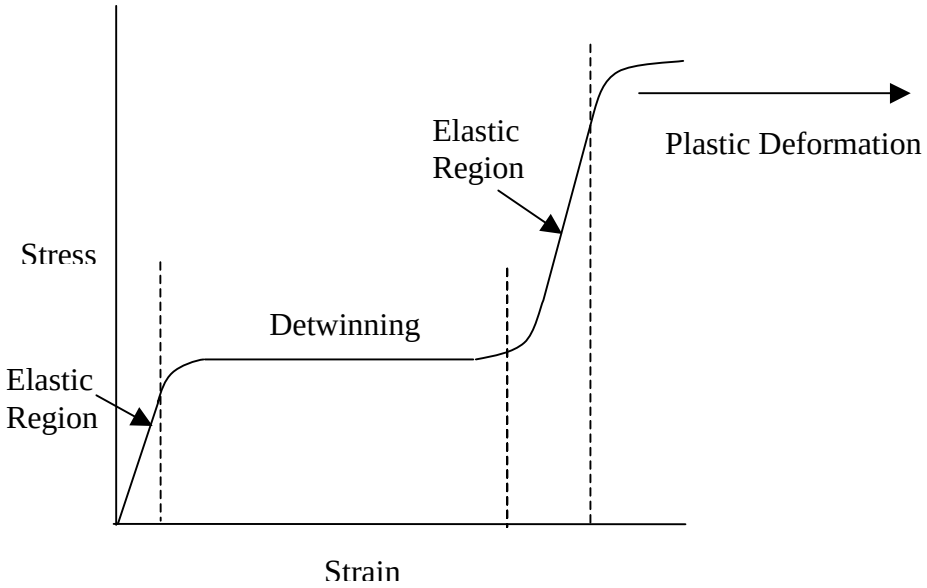

Figure 2.7: Martensite stress-strain behavior at temperatures below the martensite finish temperature.

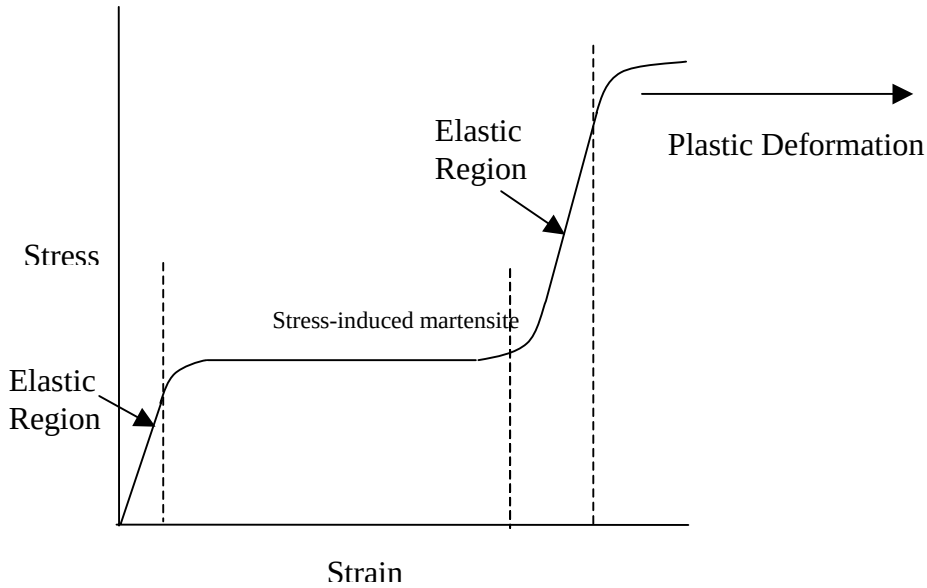

Figure 2.8: Austenite Stress-Strain Behavior at temperatures above the austenite finish temperature.

The martensite stress-strain behavior is a result of a test done below the martensite finish temperature, while the austenite stress-strain behavior is a result of a test done above the austenite finish temperature.

Looking at the martensite stress-strain behavior on Figure 2.7, it starts out with an elastic deformation region. When applying a load within this region, the SMA is able to go back to its original length without any deformation when the load is removed. To strain the material into a stable elongated state, one has to strain it into the next stage, the flat portion of the curve indicated as "detwinning." Detwinning is the reorientation of the twins until they all lie in the same direction.

Once detwinning is complete, the material goes through a second stage of elastic deformation. In and below this region, all strain can be recovered, which is critical to the design of the heat engine discussed in this thesis. Any stress applied beyond this region will plastically deform the material.

Figure 2.8 shows the austenite stress-strain characteristic. Just like the martensite phase behavior, the plot starts out with an elastic region, in its austenite phase. At the end of the elastic limit, a martensite phase starts forming while we still have the high temperature environment. This region is what we refer to the "stress-induced martensite region."

The stress of SMA in the austenite phase is about 300 times greater than the stress in the martensite phase at a given strain level. Figure 2.9 is a comparison of the strength level of the two phases.

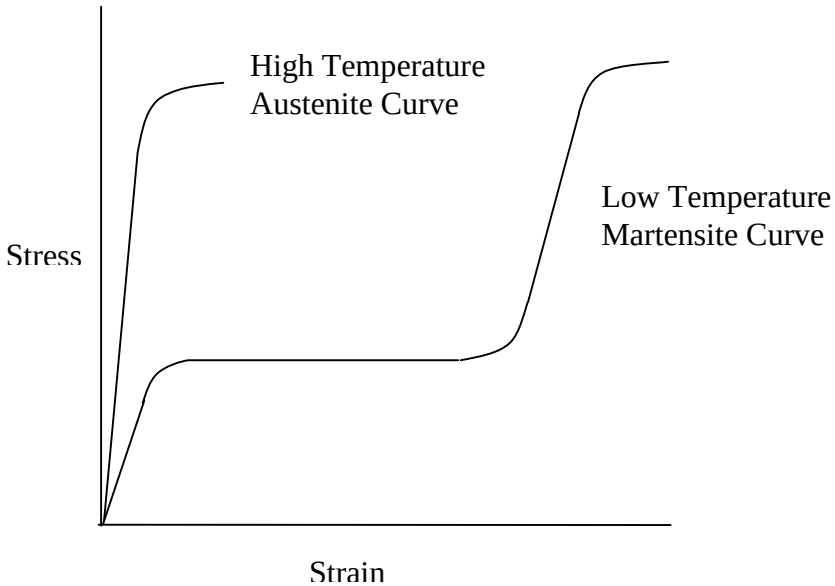

Figure 2.9: Stress-Strain Plot for comparison of the Austenite and Martensite level of stress.

Below are some properties of a Nitinol wire that might be useful for a designer. The properties presented compare the properties of NiTi and stainless steel. These properties open the way for a variety of applications that we will be considering towards the end of this chapter.

Table 2.1: Comparison of Nitinol with that of stainless steel
[http://www.sma-inc.com/nitivssteel.html]

Property	NiTi	Stainless Steel
Recovered Elongation	8%	0.8%
Biocompatibility	Excellent	Fair
Effective Modulus	approx. 48 GPa	193 GPa
Torqueability	Excellent	Poor
Density	6.45 g/cm3	8.03 g/cm3
Magnetic	No	Yes
UTS	approx. 1,240 MPa	approx. 760 MPa
CTE	6.6 to 11.0 cm/cm/deg.C	17.3 x 10-6 cm/cm/deg.C
Resistively	80 to 100 micro-ohm*cm	72 micro-ohm*cm

Applications of Shape Memory Alloys

Among hundreds of alloys that exhibit the shape memory effect, only two alloy systems, TiNi and CuZnAl, have found practical applications. Other alloys are expensive or they exert insufficient force for most applications. Nitinol, TiNi, is used almost exclusively in applications where operations are repeated many times such as electric switches and actuators (Funakbo, 176).

In 1989 a survey was conducted in the United States and Canada that involved seven organizations. The survey focused in predicting the future technology, market, and applications of SMA'a. It was meant to assist marketing managers and application

engineers in the area of SMAs. The companies predicted the following application of Nitinol in a decreasing order of importance: (1) Couplings, (2) Biomedical and medical, (3) Toys, demonstration, novelty items, (4)Actuators, (5)Heat Engines, (6)Sensors, (7)Cryogenically activated die and bubble memory sockets, and finally (8)lifting devices (Miller,17). I will describe the basic principle behind some of these applications of Nitinol in the order of their popularity, as the professionals predicted it almost two decades ago.

Couplings

Application of SMAs in the pipe fitting business started back in the 1970s. The coupling is a tube made from a SMA tube. The SMA tube is formed with its inner diameter set to 4% smaller than the outer diameter of the tubes that will be joined. The alloy is designed to have a transformation temperature far lower than room temperature (about -150^{o}C).

Before the connection, the coupling is cooled below its transformation temperature. Then it is forced to open to 7% or 8% greater than its starting size so that the two pipes can be inserted at either end of the coupling. As the coupling temperature rises to room temperature, it reverts to its original diameter, binding the ends of the pipes (Figure 2.10).

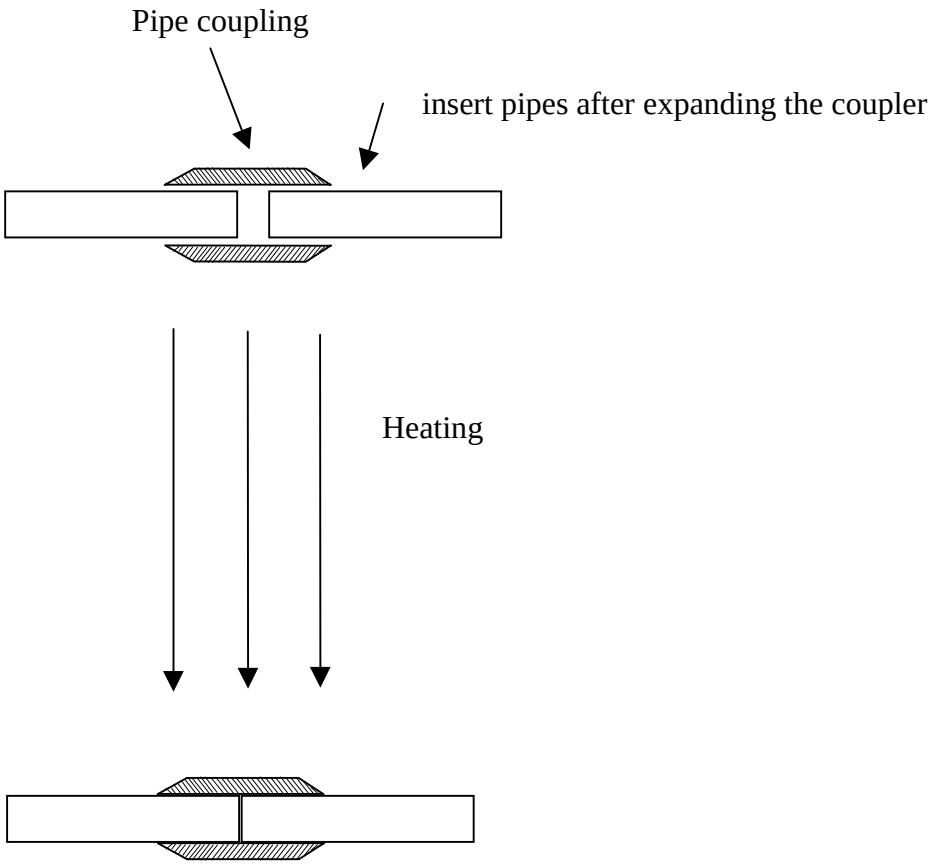

Figure 2.10:Shape Memory Alloy Pipe Coupling

"More than one hundred thousand (100,000) of these couplings have been installed in the hydraulic systems of F-14 jet fighters. They are reported to be completely free of oil leaks and other troubles." Such coupling have also found massive use in the plumbing of atomic submarines, warships, and ocean-floor oil transportation of oil." (Funakubo, 204-205).

Biomedical and Medical Applications

Shape memory alloys offer highly desirable features for the medical world, such as mechanical, chemical, and biological reliability. When foreign material is in contact with internal parts of the human body, care must be taken to insure that the material does not react with bodily tissues. Most of NiTi alloys do not react with body tissues, consequently, the potential applications of Nitinol are expanding.

Some of the applications include compression plates for internal fractures, surgical instruments, micro pumps, blood pressure test valve, and many more. I will describe two of the medical applications of Nitinol, namely its application in connecting bones and in blood clot filters.

Nitinol wires that have transition temperatures that are below the human body temperature have been used to connect bones. The wires were applied clinically by using them for connecting the greater "trochanter" and the "olecranon," Figure 2.11. The result showed that these connectors produced secure binding.

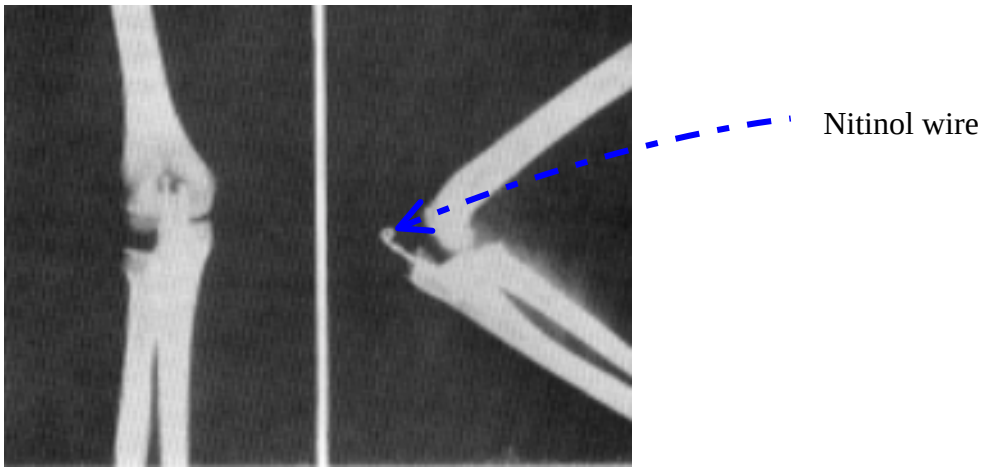

Figure 2.11: Nitinol wire used in a band for connecting bones

Another medical application is the use of TiNi in construction filters for trapping blood clots. The filters were trained initially to a shape that would allow them to trap clots. In order to insert them in blood vessels, they are stretched at low temperatures (below their transition temperature). They are inserted into the vein, using a catheter. While inside the vain, the filter undergoes phase transformation because of the body heat and reverts to its original. Figure 2.12 shows a picture of a filter inserted in the vena cava of a dog.

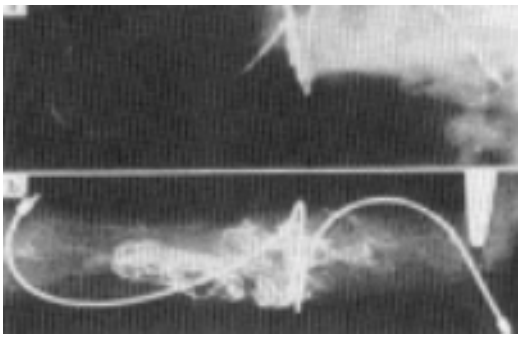

Figure 2.12: TiNi Filter inserted into the vena cava of a dog

Actuators

Actuators are another exciting application of Nitinol. Like heat engines that will be discussed in the next chapter, actuators convert heat energy to mechanical work. The difference is that heat engines undergo thermodynamic cyclic process in order to produce a positive amount of work while actuators activate a process control equipment by use of pneumatic, hydraulic, or electronic signals (Dictionary of scientific and technical terms). SMA actuators employ two distinct techniques to achieve two-way movement: a biasing method and a differential method.

The biasing technique is the most frequently used method. Figure 2.13 shows a simple dead weight load acting as a bias force on a SMA spring.

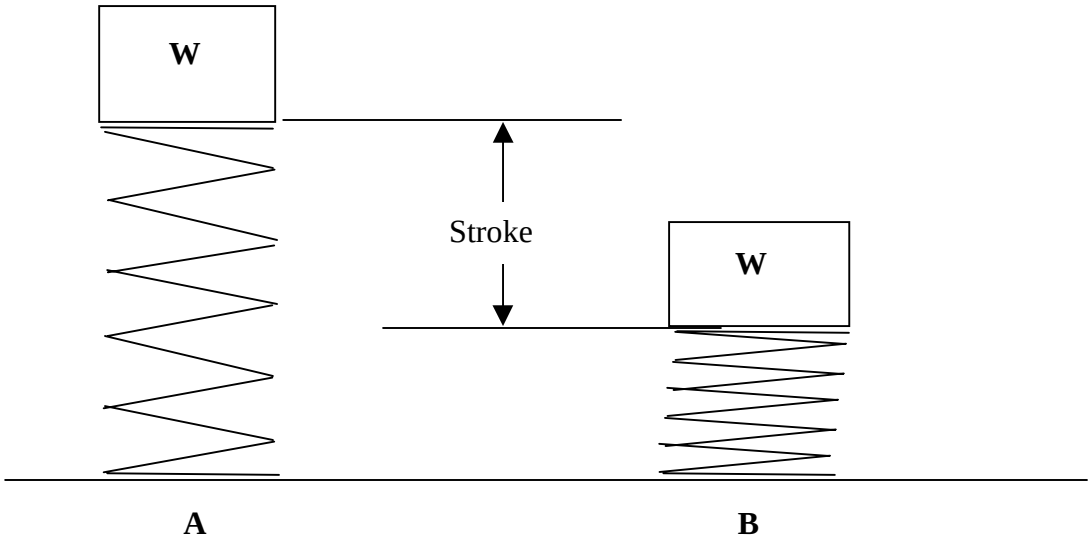

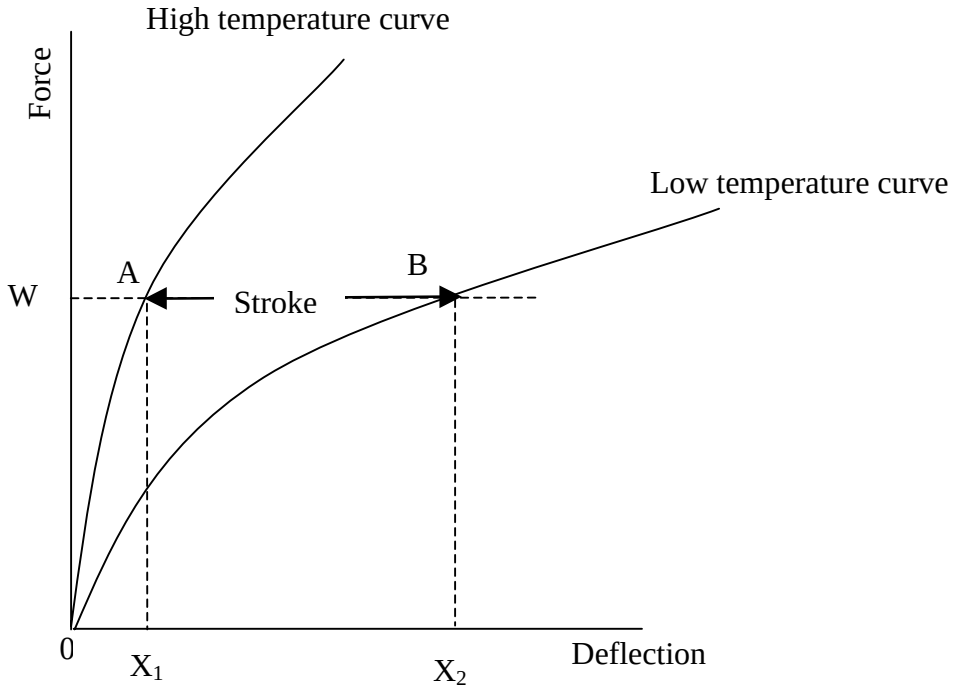

Figure 2.13: Schematic diagram of a simple two-way actuator using a dead weight bias.

Most devices use a regular steel spring instead of a dead weight as a biasing element, because a dead weight is hard to incorporate into a device.

The deflection of the spring under the bias force varies with temperature, as shown on the Figure. At temperature just higher than its austenite finish temperature, its deflection is X_1, and at temperatures below its martensite finish temperature, its deflection is X_2. That is, the spring lifts the weight, W, a stroke distance of X_2-X_1as the temperature changes between the high and low conditions. The Mars Pathfinder/Sojourner used a spring bias instead of a dead weight bias for its "material adhesion experiment" (Figure 2.14).

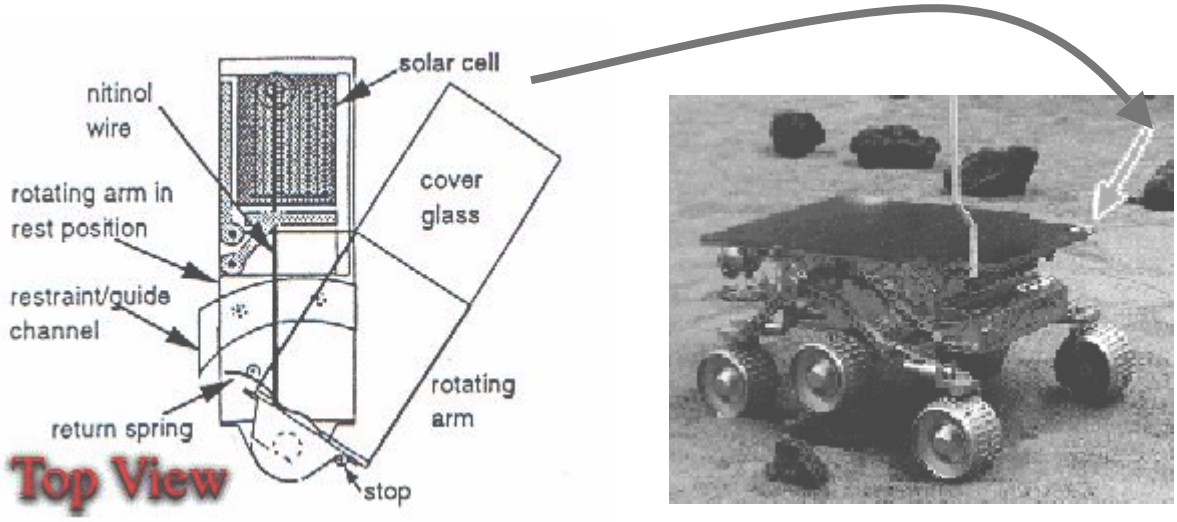

Figure 2.14: The Mars Pathfinder used a Nitinol actuation for the first time outside the earth's atmosphere [http://www.dynalloy.com/home.body.html].

The purpose of the experiment was to measure the buildup of dust on the vehicle. The experiment, located on the top front left corner of the rover, consisted of a thin glass plate mounted above a small solar cell (about the size of a postage stamp). "When commanded, the rover applies power to the SMA wire, which causes it to heat and

contract. This contraction pulls the glass plate to the side and exposes the solar cell to full sunlight. Scientists then compare the signal of the direct sunlight to the signal with the dusty glass plate in place and determine the total dust buildup. Future Mars missions will need to know the rate of dust accumulation to predict how to best use solar panels and to plan for possible cleaning" (http://www.dynalloy.com/home.body.html).

Heat Engines

The discussion of SMA heat engine designs is left for Chapter 3. We will look at some of the early heat engines and discuss their strengths and weaknesses compared to the VT1 heat engine.

Other applications

In electronics, SMAs are being developed in the makings of: micro circuit breakers, PC mount relays, chassis temperature controls, electronic locks, PC mount pilot valves, mechanical latches, sub-miniature door openers, micro manipulators, retrofit switch to relays, micro clutches, spring loaded releases, safety cutoffs, PC board temperature sensors, clean actuators, remote switch controllers, and read/write lifters.

In the automotive field, SMAs are being considered for door locks, turn signal oscillators, environmental controls, mirror controls, gear changing, triggers, pneumatic valve, remote releases, alarm devices, light fiber gates,

In household appliances, SMAs are being considered for moving louvers, safety cutoffs, spring releases, door openers, mechanical volt/current regulators,

electronic locks, cuckoo clocks, hair dryer cutoff/sensors, heater cutoff/sensors, motor protectors, box temperature control, and overheating controllers.

Other miscellaneous applications include, ultralight remote controls, mechanical scanners, camera manipulators, magnetic-free manipulator components, robotic limbs, smart materials, camera shutters, alarm devices, light fiber switches, mechanical IC's,

Chapter 3

Early Works

Introduction

There is no point in re-inventing what already exists, but knowing what has already been developed is the ladder to the next level in the development of an art. This chapter presents some of the work that has been done in the area of SMA heat engine. Heat engines are machines that are capable of converting energy that is in the form of heat to mechanical work. There are about nine distinctly different, patented, SMA heat engines, but only four will be considered in this review. Ridgway Banks developed the first invention that we will look at.

Heat Engine by Ridgway Banks [US3913326]

Ridgway M. Banks invented the first continuously operating heat engine that uses SMAs, at the Lawrence Berkely Laboratory of the University of California, in 1973. Figure 3.1 is a photograph showing the inventor and machinist Hap Hagopian, who built and assembled the parts for the Nitinol heat engine.

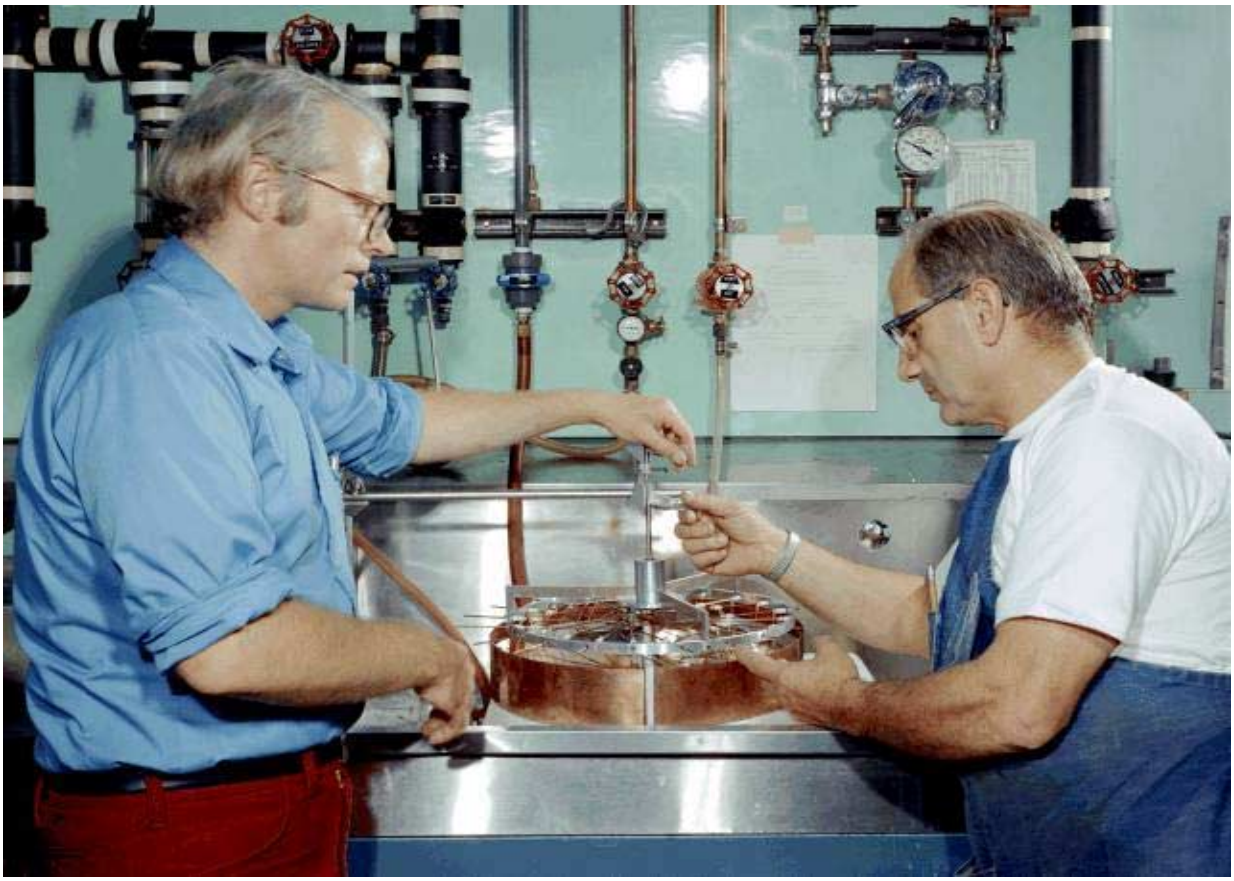

Figure3.1: The inventor Ridgway Banks and machinist Hap Hagopian working on a prototype of the first SMA heat engine(Courtesy of Ernest Orlando, Lawrence Berkeley National Laboratory)

He filled half of a small circular cylinder, about the size of a cookie tin, with hot water. He then constructed a flywheel, holding 20 nitinol-wire loops suspended from the spokes of the wheel, and set it into the cylinder. Figure 3.2 shows a top view of the flywheel.

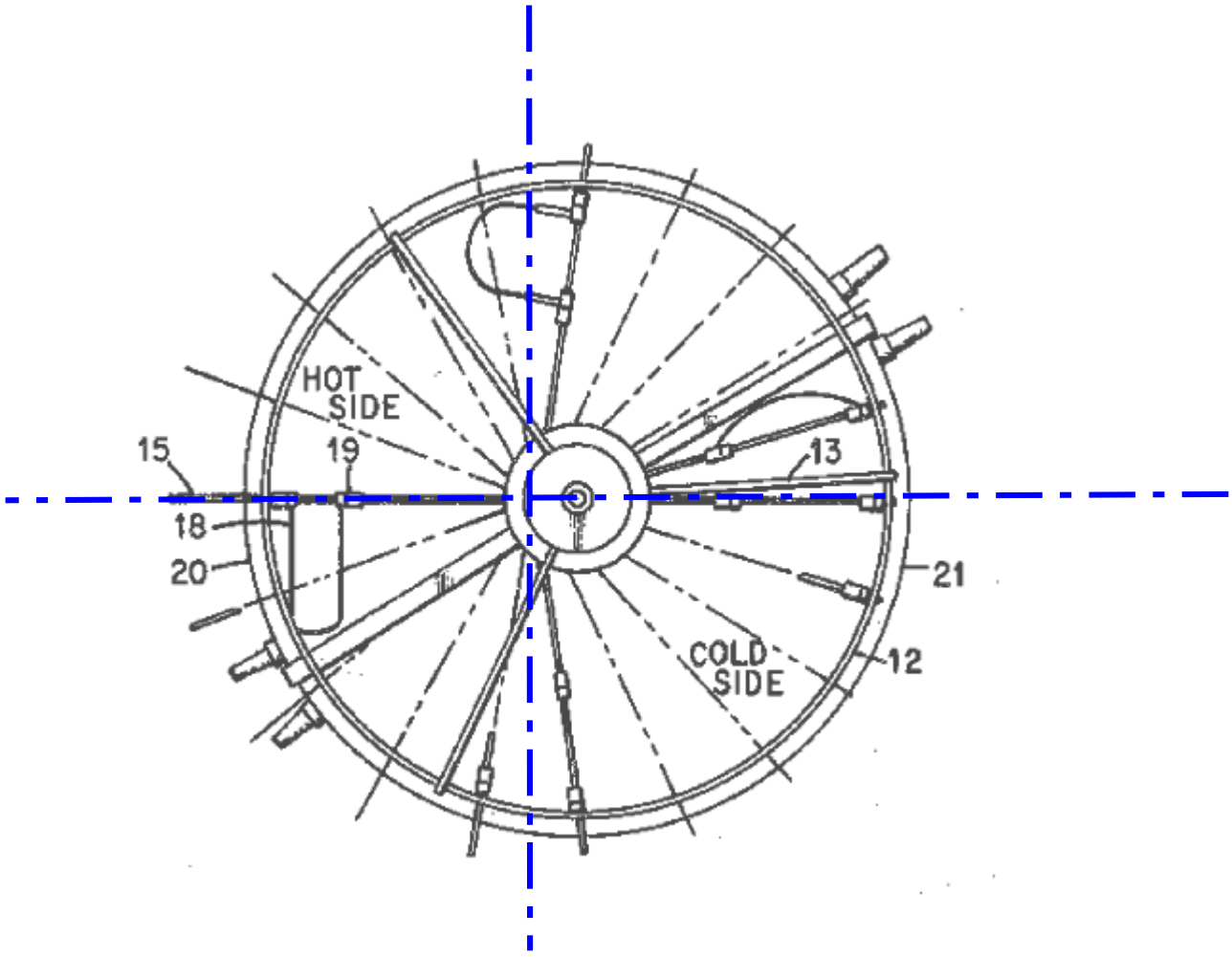

Figure 3.2: A plan view of Banks' heat engine

The wheel-hub is on an offset axis. The eccentric position of the hub causes the SMAs to stretch more on one side of the wheel than on the other." Because the nitinol loops contracted powerfully and straightened out as they went through the hot water, with a force of somewhere around 67,000 pounds per square inch, they were able to turn the flywheel, and then because they quickly assumed their original shape in the cold water bath they were able to exert their force again when they hit the hot-water side. The wheel thus could run continually providing energy of up to about 70 rpm and capable of generating about half a watt of electricity" (http://mai.flora.org/forum/1841).

This device operated to more than 23 million cycles with the original wires intact, but it had inherently inefficient use of nitinol wire, because the system did not employ uniaxial deformation, which provides larger power densities and efficiencies. Not only that, but it also suffered "substantial mechanical and thermal parasitic losses due to hydrodynamic friction" (IECEC, 1981, 185).

The engine's thermodynamic inefficiency comes from the fact that the engine's cold Nitinol elements are heated by immersion in a hot fluid and then the elements get cooled in a heat sink at a much lower temperature. Such extreme temperature differences are a source of irreversibility, because of the large amount of entropy generated. Therefore, the engines cannot approach the efficiency of an ideal engine, or Carnot efficiency. Chapter 7 provides a more complete thermodynamic analysis of SMA heat engines.

Heat Engine by Alfred Davis Johnson [US4055955, 1977]

Dr. Johnson is one of the early inventors of SMA heat engines. He now has a different interest; his company manufactures micro-valves, a growing field in the SMA market. He built his first heat engine in 1976, a couple of years after Mr. Banks invention.

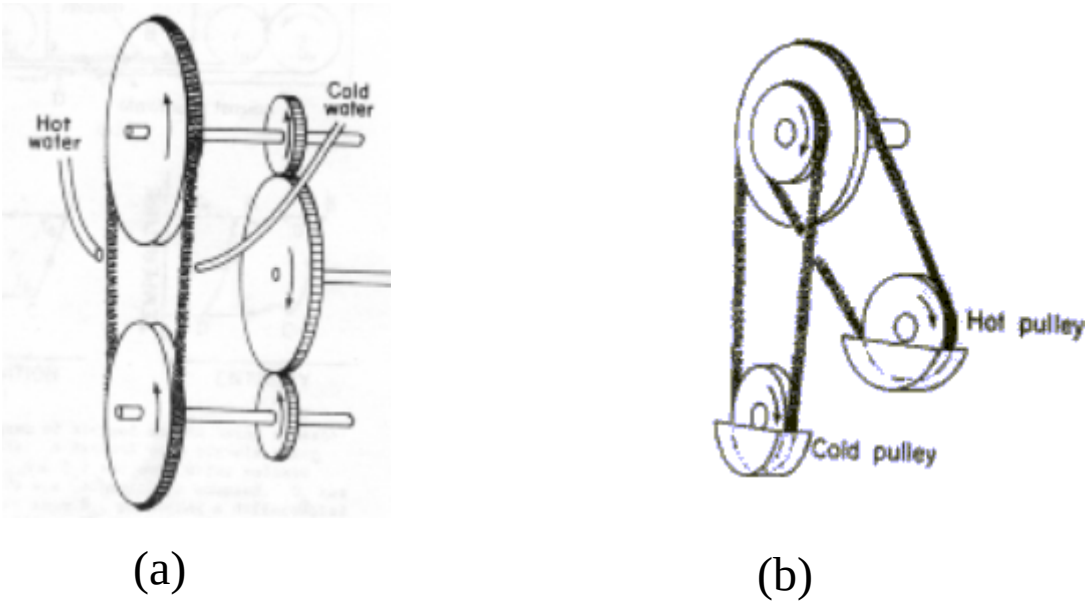

Figure 3.3: a) Johnson's engine using nitinol in the form of a continuous helix, synchronized using gears.
b) A modified form of engine "**a**" Here, one large and one small pulley fixed on the same shaft, synchronized as they rotate.

He built two kinds of engines shown in Figure 3.3. In Figure 3.3a, Johnson's engine includes a SMA coil made into a non-slip engagement (grooved pulley) about a

pair of small and large diameter pulleys, mounted in a heat source and heat sink. The pulleys rotate in one direction, at the same angular velocity by gears, which synchronize them. The conjoint rotation makes the cold wire portion to stretch, and thereafter, the heated portion of the wire contracts to its memory-shape during its movement past the heat source. The difference in tension between the two portions of the coils result in a net torque on the larger diameter pulley, which produces power output.

In Figure 3.3b, we see that the setup of the coil is in such a way that the inner and outer sets of pulleys mount on a common shaft that run to a heat sink and a heat source, respectively. The pulley in the heat sink is of a larger diameter than the pulley in the heat source. The pulleys are constrained for rotation in a clockwise direction.

"The efficiency of these helical-band engines is certain to be low, because water is readily transported by the helix so that the hot and cold reservoirs are rapidly mixed" (IECEC '75). In addition, although Mr. Johnson may not have realized it, the design of this engine requires the coils to slip or jump teeth relative to the pulleys. This also reduces the overall efficiency of the device.

Heat Engine by John J. Pachter [US1975000732471]

Pachter's work, like Johnson's engine, is similar to the engine presented in this paper. He uses continuous SMA belt, lengthened and shortened at different portions by thermal means. The belt is wrapped around a pair of pulleys of different diameters, one pulley being of slightly smaller diameter than the other is. The pulley shaft of each pulley then connects to the shaft of another pulley.

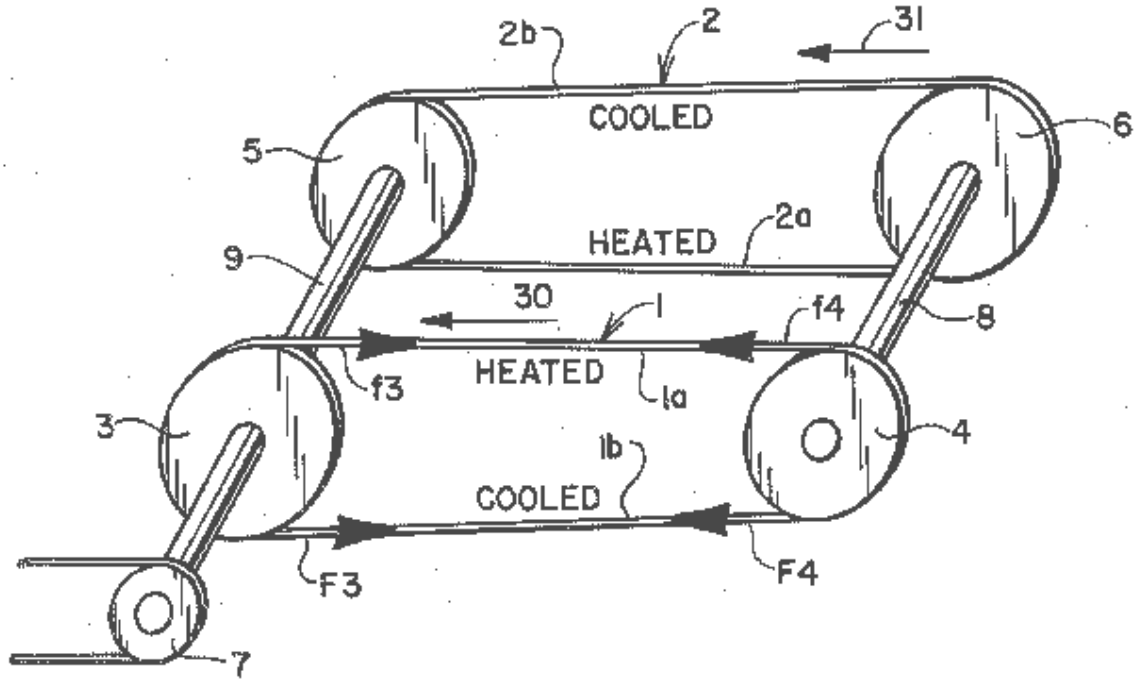

Figure 3.4: A simplified representation of Pachter's engine

The rotation of the pulleys required heating and cooling of selected portions of the belts. Belt 1 causes pulleys 3 and 4 to rotate in the direction of arrow 30 as heat is applied to region 1a and region 1b is cooled. Similarly, belt 2 causes pulleys 5 and 6 to rotate in the direction of arrow 31, which is in the same direction as arrow 30 by applying heat in region 2a and removing heat from region 2b. Finally, the shaft rotation passes on to an external object via pulley 7.

Having two sets of pulleys whose belts are heated at alternate locations is responsible for generating a continuous rotation. The connection prevents reverse rotation of the pulleys with respect to each other. Like Johnson's device, this engine also requires slip between the belt and the pulleys in order to function. This slip reduces efficiency and probably results in erratic operation.

The heat engine, presented in this thesis work, accounts for the slip that is present in Johnson and Pachter designs. The next chapter will present a proposed design that is currently under construction, the VT1 heat engine.

Chapter 4

Design of the VT1 SMA Heat Engine

Introduction

The VT1heat engine is a simple device with few moving parts. It operates directly upon the application of heat to a portion of the SMA wire chain. Its purpose is to convert heat energy to useful work while executing a cycle. Figure 4.1 is a photograph of the test rig, at an intermediate stage in the development of the engine. The thermodynamic and the mechanical modeling of the engine, presented in Chapter 5 and 6 respectively prove, at least in theory, that the engine can work. This chapter presents the design of the heat engine with drawings of each part, detailed description of each part, and some of the problems associated with the design or implementation of each part.

We will start of by discussing the entire engine assembly as a single unit, then we will go on to describe individual parts. The intent of this chapter is to provide all the design information needed by someone trying to understand or improve upon on the current design.

The Assembly

Normally, a chain driven system transmits power from one rotating shaft to another. The VT1 SMA heat engine transmits power from the SMA chain to two rotating shafts. The design consists of a SMA driving roller-chain, two driven plastic sprockets whose teeth engage the rollers of a SMA chain, a synchronizer chain, and other components described in the following sections (figure 4.1).

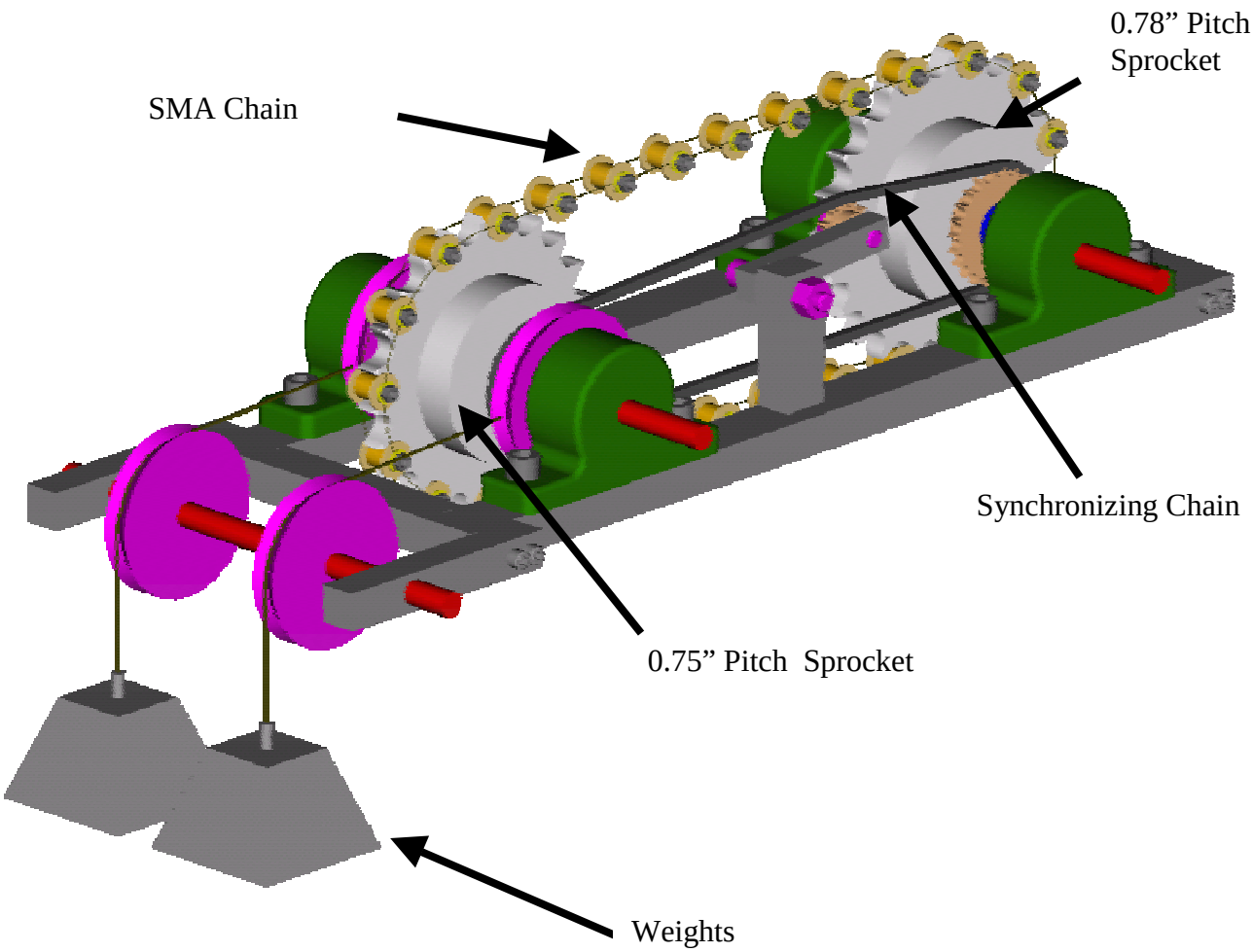

Figure 4.1: 3D Representation of the VT1 heat engine assembly

The basic idea behind this specific design is similar to the Johnson heat engine described in chapter 3. Like the Johnson's design, there is a heat source, a heat sink, an actuating band and a synchronizer (the heat sink and heat source are not shown in the figure above). Unlike the Johnson and Pachter designs, however, this concept uses a roller chain with SMA links as the band mechanism in an attempt to eliminate the inherent slip found in the Johnson device. The figure shows a 3D model of the design with the major components labeled.

The chain, constructed from a SMA, needs to be stretched, on the top and bottom portions, to 2% of its original length, as a start up requirement. When the top part of the chain is heated, it will contract back to its original shape while stretching the cold section of the chain by another 2%. With a 4% strain, the cold section of the chain will have a 0.78in pitch, which is equal to the pitch of the sprocket on the left; the sprocket on the right has a 0.75in pitch. Heating the top part of the chain and cooling the bottom part creates an overall torque that tends to turn the sprockets clockwise. The static and dynamic model discussed on the next chapter will show this to be true.

The two plastic sprockets are designed to have different pitch and number of teeth. The resultant torque is generated as a result of having these differences. On the other hand, the synchronizer sprockets must have the same number of teeth, because the purpose of the synchronizer is to force the plastic sprockets to rotate at the same speed. As a result, the plastic sprockets must have slightly different pitches to accommodate the expansion and contraction of the SMA wire. The concept will become clearer when we look at the progressive development of the final design in the next chapter. In this chapter, I will present a brief description of the components of the VT1 heat engine, starting with the heart of the design, the SMA chain.

The SMA Chain

The SMA chain concept is a novel feature of this design as far as we can tell from public records of the U.S. patent office. Its construction is similar to standard single strand type roller chains. Therefore, the construction of this chain uses the standardized specifications for roller chains, as set forth by the American Standards Association, ASA (Standard B29.1-1950). The ASA standard chain number that we based our design is chain number 60.

The chain is made up of rollers, spacers, pins and link plates (Figure 4.2). In this design, the link plates are replaced by shape memory wire and stainless steel washers. According to the *Design Manual for Roller and Silent Chain Drives* (Jackson and Moreland, 34) any roller chain can be identified by three parameters: pitch, chain width, and roller diameter.

The pitch of the roller chain is the distance, in inches, between the centers of adjacent joint members. All standard roller chains are pitch proportioned, i.e., pitch is the dimension on which the other dimensions for standard chains are based.

Chain width (sometimes called nominal chain width) is the minimum distance between the link plates of a roller link, and is approximately 5/8 of the pitch.

A 3D drawing of the roller assembly is shown in figure. 4.2. It consists of rollers that are evenly spaced, 1.5in apart, throughout the chain. Although the pitch of the sprocket is 0.75in, I chose to have 1.5in distance between the rollers, because this allows enough material to be exposed for heat transfer. If there was only 0.75-inches inter-roller distance, the rollers will be so close to each other that there might not be enough SMA wire length to induce effective actuation. Because of this change, the rollers engage the sprockets on every other tooth.

Roller-Chain Assembly

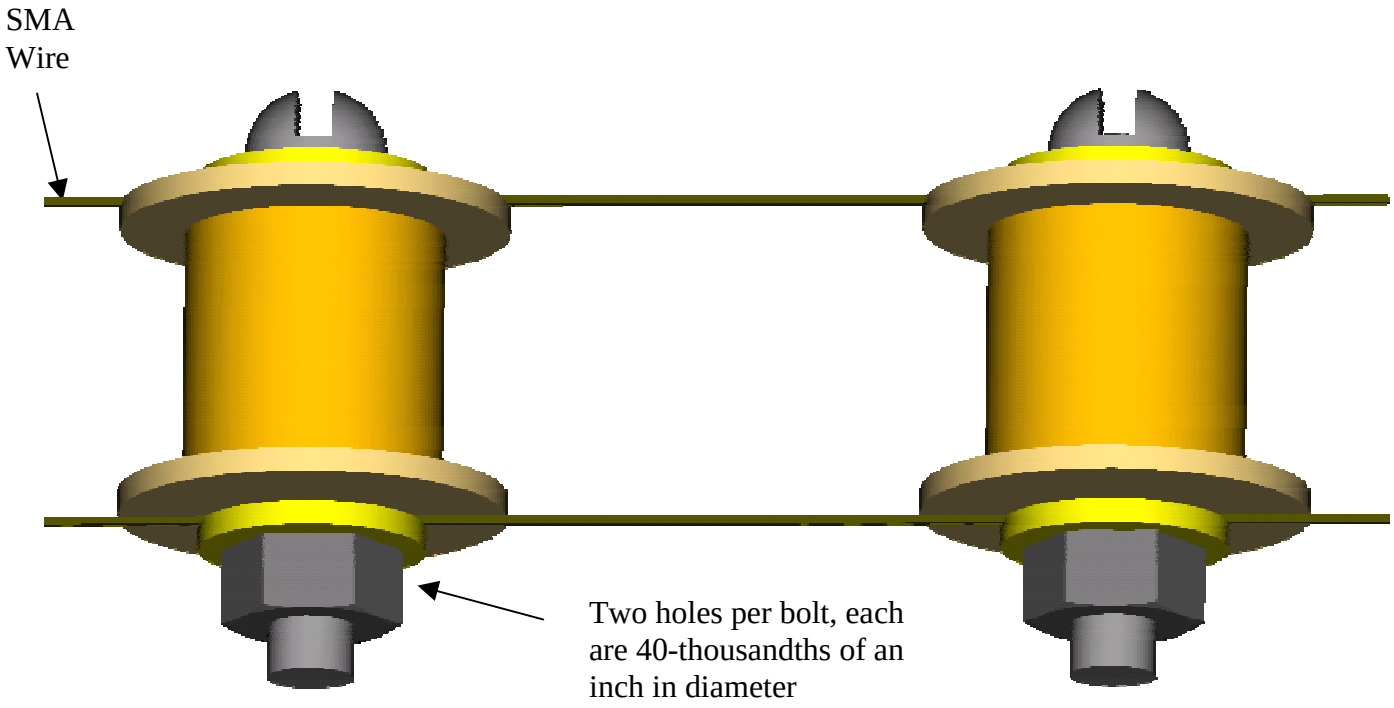

Figure 4.2: 3D CAD drawing of the SMA roller chain assembly

The first component of the assembly is the roller, which is made of nylon. Nylon was used because it has low friction in the absence of lubrication and it is lightweight. It is 0.5 inches wide, with inside and outside diameters being 0.252 and 0.5-inches, respectively. These dimensions allow the roller to engage easily onto the sprocket and roll, on its axis, with minimum resistance.

The next component of the roller-chain assembly is the spacer. This design used a 5/8-inch long aluminum tube with its inside and outside diameters being 0.166-inch and

0.25-inch diameter, respectively. The 0.25-inch outside diameter is 2-thousandths of an inch less than the inner-diameter of the roller, which allows the spacer clearance to rotate within the roller.

The inside diameter, 0.166-inches, is also 2-thousandthse of an inch larger than the outside diameter of the pin that runs through it. In this case, the pin is made from an aluminum screw.

The Pin

The screw, which was used for the pin, was the most challenging of all the parts, in terms of machine work. It is an 8-32, aluminum, flat head screw. Two transverse 0.040-inch diameter holes must be drilled through this screw to accommodate the wire, as shown in figure. 4.2. These transverse holes were difficult to drill. Initially, I planed on using steel screws, because steel would be stronger. Unfortunately, steel proved to be difficult to drill and rapidly consumed drill bits. For this reason, the steel screws were replaced by aluminum screws, even though the steel would have been preferred for strength and durability.

Such small holes are hard to drill accurately. In fact, as I will explain in a later chapter. To save time and to increase accuracy, the holes were drilled with the help of a fixture, shown in figure 4.5. The fixture was made from steel, machined to a one-inch by one-inch square block.

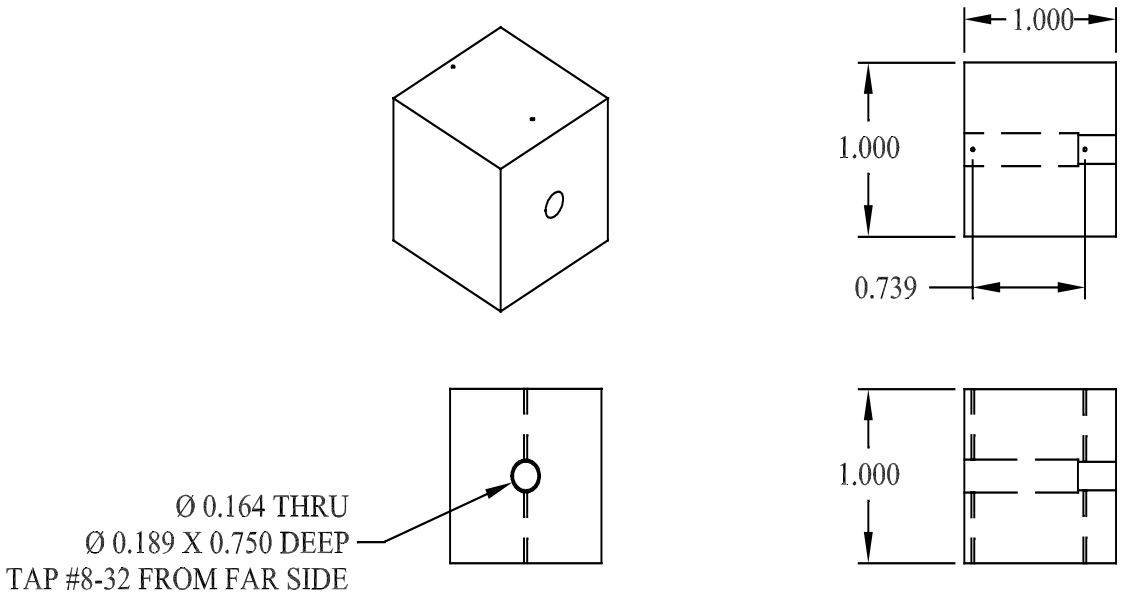

Figure 4.3: AutoCAD drawing of the fixture that holds the aluminum screw in place during machining.

The block has a larger hole with a threaded end that serves as a fixed point for the aluminum screw that needs to be drilled at the two locations shown in Figure 4.4. The block has two 40-thousandths diameter holes drilled transverse to this large hole. The chain in this design has 28 rollers. This means that 28 cross-drilled screws are also needed.

The SMA Wire

The shape memory wire is the actuating material. Initially, the design used a nitinol actuator wire with a transition temperature that was below room temperature. This made it difficult to work on the wire, because at temperatures higher than the transition temperature, the alloy is harder and less ductile. This wire was replaced by a second nitinol with a higher transition temperature. Finally, to improve the actuation displacement, we replaced the nitinol wire by another type of SMA wire known as Flexinol.

Flexinol actuator wire, unlike other SMAs, it works better in extension/contraction applications, because compared to other SMAs the crystals are better aligned. The wire can be used for tens of millions of cycles if used within the manufacturer's guidelines (www.dynalloy.com). One must be careful when using the wire, because permanent deformation of the wire can occur as a result of high stress and temperature. Excessive heat, as high as 400^{o}C (annealing temperature of Nitinol) could result in a loss of the memorized shape. If higher strains are imposed (more than 5%), then the memory strain is likely to slowly decrease and good motion may be obtained for only hundreds or a few thousand cycles.

As can be seen in Figure 4.2, two sets of wires are firmly fixed in parallel on each side of the screw. You can also see that two sets of washers, one on each side of the screw, protect the wire from damage during motion. A single nut, made from steel, compresses the wire between the washer and the aluminum spacer.

In order to approximate the amount of wire needed, the total chain length is calculated based on Jackson and Moreland's approach (Jackson and Moreland, 50). The approximation is done for a given center to center distance and a given sprocket size. The authors suggest, for simplicity, to compute the chain length in terms of chain pitches, and then to multiply the result by the chain pitch to obtain the length in inches. For this reason, we will assume that the chain has a uniform pitch, which is 0.75in, even though the chain-pitch will change during operation. Please not that, though the sprockets are represented here as having large difference in diameter, the actual sprockets are similar in size, Figure 4.4. The exaggerated differences are meant to help the reader understand the concept clearer.

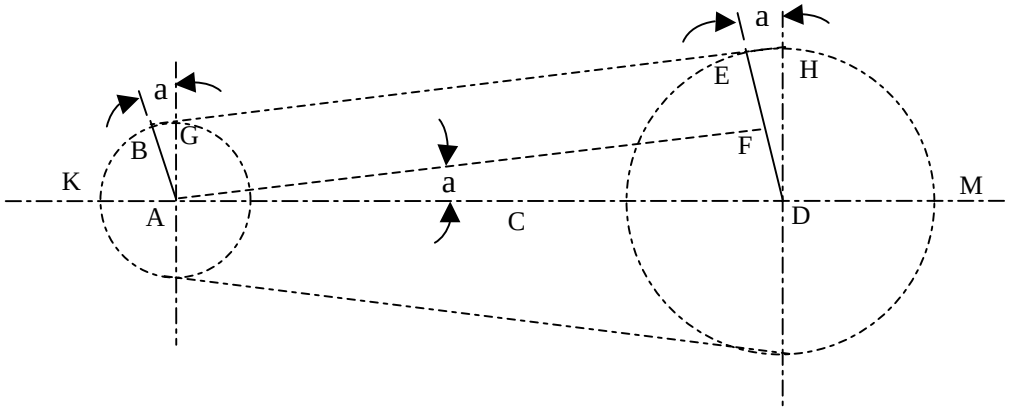

Figure 4.4: Sketch for computation of chain length

The pitch radii of the two sprockets expressed in chain pitches are

$$DE = \frac{1}{2\sin\left(\frac{180^0}{N}\right)} \qquad \textit{Equation (4.1)}$$

$$AB = \frac{1}{2\sin\left(\frac{180^0}{n}\right)} \qquad \textit{Equation (4.2)}$$

where, N and n are the number of teeth in the large and small sprockets.

The tangent length, BE is given by,

BE = AD cosine (a) = C cosine (a) *Equation (4.3)*

Where, C is the center distance expressed in pitches.

Angle 'a', in degrees, is

$$a = \sin^{-1}\left(\frac{DF}{AD}\right) = \sin^{-1}\left(\frac{DE - AB}{AD}\right) \qquad \textit{Equation (4.4)}$$

Substituting Equation 4.1 and 4.2 into Equation 4.3,

$$a = \sin^{-1}\left[\frac{\frac{1}{\sin\left(\frac{180^0}{N}\right)} - \frac{1}{\sin\left(\frac{180^0}{n}\right)}}{2C}\right]$$ *Equation (4.5)*

One-half the length of the chain wrapped on the large sprocket, arc ME, measured in chain pitches, is,

$$ME = MH + HE = \frac{N}{4} + N\frac{a}{360^0}$$ *Equation (4.6)*

Similarly, one-half the chain wrapped on the small sprocket is,

$$KB = KG - BG = \frac{n}{4} - n\frac{a}{360^0}$$ *Equation (4.7)*

Then if L is the entire length of chain in pitches, assuming that there is no slack in the system,

L =2 [BE + ME + KB] *Equation (4.8)*

Substituting Equations 4.3, 4.7, and 4.8, into Equation 4.8,

$$L = 2\left[C\cos(a) + \frac{N+n}{4} + \frac{a}{360^0}(N-n)\right]$$ *Equation (4.9)*

Rearranging the formula,

$$L = 2C + \frac{N+n}{4} + \frac{C}{N-n} * \left[\frac{a}{180^0} - \frac{2C(1-\cos(a))}{N-n}\right]\frac{(N-n)^2}{C}$$ *Equation (4.10)*

but, Jackson and Moreland suggest, the term

$$\left[\frac{a}{180^0} - \frac{2C(1-\cos(a))}{N-n}\right]\frac{(N-n)^2}{C},$$

can be replaced by $\frac{1}{4\pi^2}$

Thus,

$$L = 2C + \frac{N+n}{2} + \frac{(N-n)^2}{4\pi^2 C}$$ *Equation (4.11)*

Since N = n,

L=2C+N *Equation (4.12)*

Since the SMA chain changes its pitch with temperature, this formula (Equation 4.12) is only an approximation. Therefore, the length of the SMA chain for standard chain and sprocket sets is two times the center distance plus the sprocket number of teeth.

The current rig has a center to center distance that is about 12-inches, which is equivalent to about 16 chain pitches, assuming a 0.75-inch pitch.

Therefore the chain length is,

$L \approx 2\ (16) + 23$ chain pitch

$L \approx 55$-chain pitch

This is equivalent to,

$L \approx 55 * 0.75$-inches

$L \approx 41.25$-inches.

Hence, the approximate length of wire needed when constructing the chain is 82.5-inches, since the chain requires a wire on either side of the rollers.

The Sprockets

The pitch, chain width, and roller diameter determine the dimensions of the sprockets with which the roller links must engage. The sprockets used had two different teeth numbers, for the first design; one 23 and the other 24. As the design progressed, both sprockets were made to have the same number of teeth, 23, but different pitch. The difference in pitch was the limiting factor of the strain.

Stretching above the elastic limit of the chain will cause damage to the device. Most SMAs can recover strains as big as 8%, under zero loads. Manufacturers suggest that the strain should be limited to about 4% and the pull force should not be greater than 25ksi. These limitations insure longer cycle life and better performance.

Another feature that characterizes the sprocket is a 1-inch diameter hole at its center. Through this hole runs an aluminum shaft with inner diameter of 0.5-inch and an outside diameter of 1-inch. This shaft serves as a spacer that separates the bearings. A second shaft with a diameter just under 0.5 inches runs through this outer shaft. This latter shaft runs through a pair of bearing that are firmly fixed to the frame. As can be seen from figure 4.1, the shaft sticks out of the bearings. This is done to allow torque measurements once the engine is in operation.

In this section, we will look at the calculation that went into the design of the sprocket with the 0.78in pitch. This design calculation was needed, because a 0.78in pitch is non standard and no manufacture carried a sprocket with such pitch. The calculation provides values for the parameters in figure 4.5 that define the profile of the sprocket (Binder, 7).

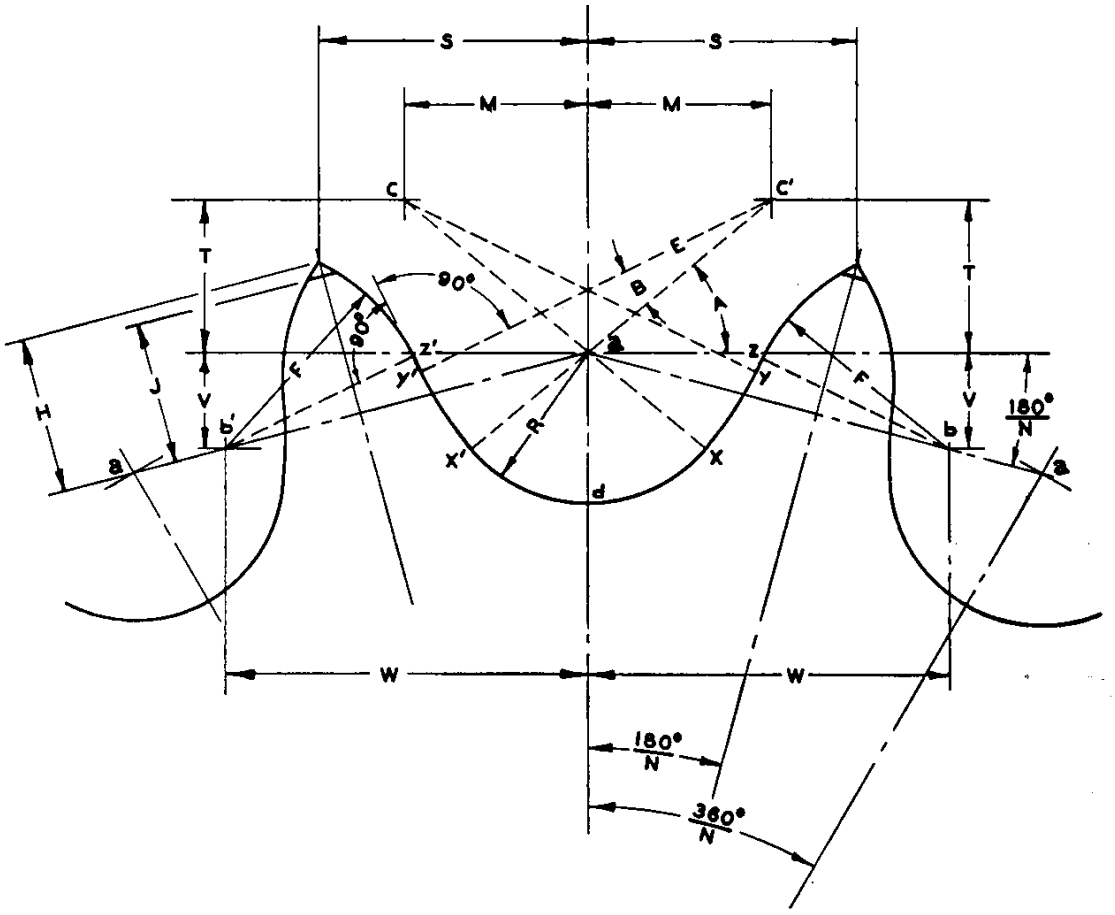

Figure 4.5: Standard sprocket tooth form for roller chains.

Let: P = pitch = 0.78in

N = number of teeth =23in

D_r = nominal roller diameter = 0.5in

D_s = seating curve diameter

$$R = \frac{Ds}{2} = 0.5025D_r + 0.0015 = 0.5025(0.5) + 0.0015 = 0.25275\text{in}$$

$D_s = 2R = 2(0.25275) = 0.5055in$

$A = 35^o + 60^o/N = 35^o + 60^o/23 = 37.61^o$

$B = 18^o - 50^o/N = 18^o - 50^o/23 = 15.83^o$

$ac = 0.8D_r = 0.8(0.5in) = 0.4in$

$M = ac\ Cos(A) = 0.4\ Cos(37.61) = 0.317in$

$T = ac\ Sin(A) = 0.4\ Sin(37.61) = 0.244in$

$E = 1.3025D_r + 0.0015$

$Chord\ xy = (2.605D_r + 0.003)Sin(9^o - 28^o/N)$

$= (2.605(0.5) + 0.003)Sin(9^o - 28^o/23) = 0.1768in$

$Length\ of\ line\ between\ a\ and\ b = 1.24D_r. = 1.24(0.50) = 0.62in$

$yz = D_r\ [1.24Sin(17^o - 64^o/N) - 0.8Sin(18^o - 56^o/N)]$

$= 0.5\ [1.24Sin(17^o - 64^o/23) - 0.8Sin(18^o - 56^o/23)] = 0.0449in$

$Angle\ which\ the\ line\ ab\ makes\ with\ horizontal = 180^o/N = 180^o/23 = 7.826^o$

$W = 1.24D_rCos(180^o/N) = 1.24(0.50)\ Cos(180^o/23) = 0.614in$

$V = 1.24D_rSin(180^o/N) = 1.24(0.5)\ Sin(180^o/23) = 0.0844in$

$F = Dr[0.8Cos(18^o - 56^o/N) + 1.24Cos(17^o - 64^o/N) - 1.3025] - 0.0015$

$= 0.50[0.8Cos(18^o - 56^o/23) + 1.24Cos(17^o - 64^o/23) - 1.3025] - 0.0015$

$= 0.3336in$

$$H = \sqrt{F^2 - (1.24D_r - \frac{P}{2})^2}$$

$$H = \sqrt{0.334^2 - (1.24(0.5) - \frac{0.78}{2})^2} = 0.2422in$$

$S = P/2\ Cos(180^o/N) + H\ Sin(180^o/N)$

$= 0.78/2\ Cos(180^o/23) + 0.2422\ Sin(180^o/23) = 0.4193in$

When J is 0.3P, which is the case for the VT1 design, the approximate outside diameter of sprocket is

$P\ (0.6 + Cot\ 180^o/N) = 0.78(0.6 + Cot\ 180^o/23) = 6.1429in$

Thus, the sprocket with a pitch of 0.78in is designed based on the above parameters.

The technical drawing for the sprocket is shown in Appendix B.

Synchronizing Chain

The purpose of the synchronizing chain is to force the two sprockets turn at the same speed. Chapter 5 details why we need a synchronizer based on the previous designs we attempted. A regular 0.5in pitch roller chain and 20 tooth steel sprockets were purchased for synchronizing the two plastic sprockets. Unlike the SMA chain, the synchronizing chain is relatively rigid, meaning it doesn't stretch easily. But, we need to allow some flexibility for sprocket B, figure 4.5, to move freely side to side, while maintaining tension on the synchronizing chain. We can remove the slack from the chain by using an idler, figure 4.1.

Straining the SMA chain

As mentioned earlier, the roller-to-roller distance is 1.5in, which is based on a 0.75in pitch-chain-design specification. Initially, half of the chain had lengths that were 4% less than 1.5in; i.e., 1.47in. These shorter links were then strained to the 1.5in length. A later section describes the straining method used for this experiment.

In this section, I will describe the method of straining the chain. There is another method, other than the one described here, that I attempted at an early stage of the design; it will be discussed in Chapter 5. The method described here requires the sprockets to be pulled apart using weights that are hanging from a bracket that extends from the frame, figure 4.1.

To help us see the method of operation better, refer to figure 4.6. We see that sprocket A is sitting on a fixed axis, while sprocket B is sitting on a moving axis. We do

this to allow sprocket B to move, perpendicular to the axis of rotation, with respect to sprocket A when gravitational force is applied on sprocket B.

According to manufacturers of the SMA wire, a Flexinol wire takes 7-10,000 lb/in^2 to strain it to 4% of its original length. According to our design, the chain needs to be strained to about 2% as a start up condition. What I mean by "start up condition" is that any time the engine stops working for some reason, say for maintenance, the engine should start cranking, on its own, as long as there is a temperature difference between the top and bottom portions of the chain. We do this by hanging weights that strain the chain to 2% of its original length while it is in a shut-off mode (figure 4.6). When heating the top part of the chain, the top chain contracts back to its original length straining the bottom by a further 2% to an overall strain of 4%.

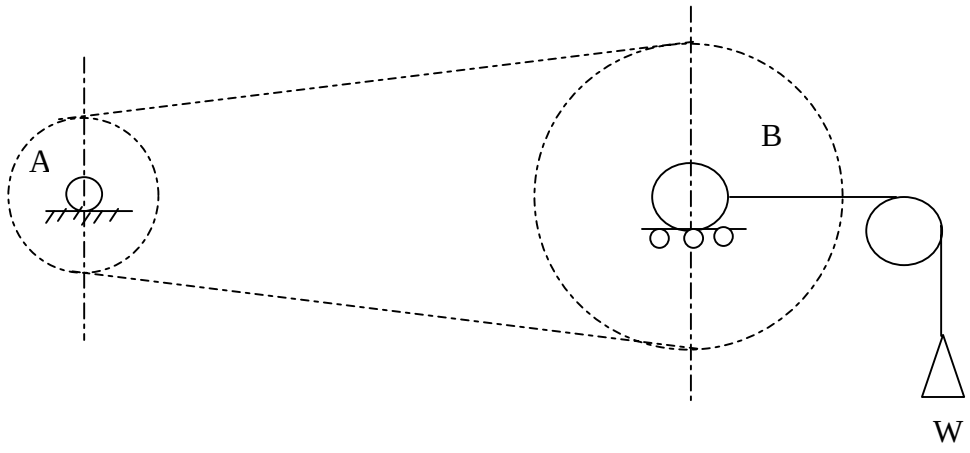

Figure 4.6: Sketch for demonstrating method of straining

The weight is calculated assuming it takes 4,000lb/in^2 to strain a single wire by about 2%. Each side of the chain, top or bottom has a pair of wires. For calculation purposes, we take it that there are four parallel wires supporting a weight, W (figure 4.7).

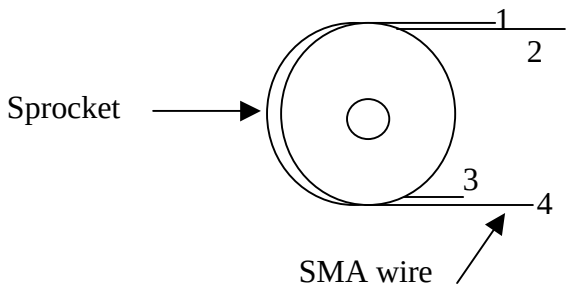

Figure 4.7: Sketch of sprocket showing the four wires that are part of the SMA chain

Therefore,

$4{,}000\ \text{lb/in}^2 = W_1/A$

Where: W_1 = the weight that needs to be applied on a single wire

A = cross-sectional area of the wire

$W_1 = 4{,}000\ \text{lb/in}^2\ A$

$A = (\pi/4)D^2 = (\pi/4)(0.015)^2 = 1.767*10^{-4}\text{in}^2$

$W_1 = 4{,}000\ \text{lb/in}^2\ (1.767*10^{-4}\text{in}^2) = 0.7068\text{lb}$

Since, we have four wires, the total weight, W, that the wires can support is,

$W = 4W_1 = 4(0.7068\text{lb}) = 2.827\text{lb}$

We need two weights on either side of the sprocket, as shown on figure 4, each weighing half of W, that is 1.414lb.

We couldn't pursue the project to completion and get to a working model, because of time. Work orders are in place to finish up the project, but it is likely that the parts will not be in before the end of this thesis. I intend to include a memo, at the end of this thesis, after the completion of the model. For now, I will describe the development of the heat engine in the next chapter.

Chapter 5

The Progressive Design of the VT1 Heat Engine

Introduction

Chapter 4 presented the final design of the VT1 SMA heat engine. This chapter will present some of the earlier work that led to this final design. Although the general concept of the heat engine was clear at the outset, several errors were made in attempting to realize a working prototype. It is hoped that, by presenting this background, the reader will gain a better understanding of the overall design and many of the subtle details that must be understood before a working prototype is possible. The presentation includes static and dynamic models, which helped to convince the researcher that the design was feasible.

At the "embryonic" stage of the design, we developed the logistics behind a simple heat engine that implemented a set of pulleys. We discovered that such engine is already in existence, so we proceeded with the idea of implementing sprockets instead of pulleys. This idea appeared appealing, because it results in a device that no longer depends on friction to produce power. We proposed that the pulleys in Johnson's heat engine can be replaced by a set of sprockets and the operating principles should still apply.

The motivation was that the sprocket-type design would not have the problem of slip and the large friction losses that are associated with the pulley-type of design. Thus,

the sprocket-type design would allow us to transmit large torque with minimum loss. The pulley type design failed in all prior prototypes when large-scale productions were attempted. The sprocket-type design might overcome this pitfall, because unlike the pulley type engines it does not require friction to transmit the motion.

Initially, we will model the pulleys as two circular bodies on which run two sets of cables; one cable represents the SMA chain and the other represents the synchronizing chain. This model is shown in figure 5.1 below. We will then draw free body diagrams of each moving body and analyze the resultant torque. Eventually, the same analysis will be extended to the sprocket/chain type design.

Pulley-type Design

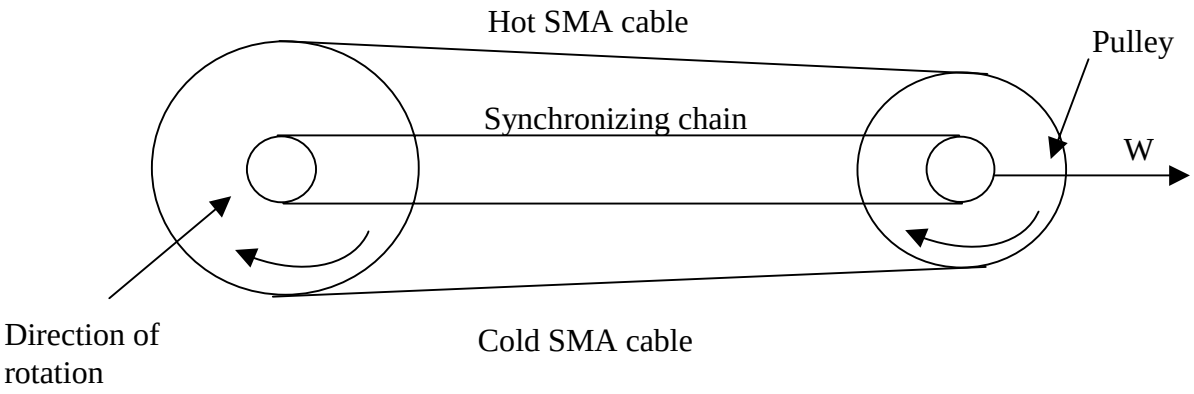

Figure 5.1: Sketch of the VT1 Nitinol Heat Engine that uses pulley-type design

Static Model

Figures 5.2 a and b are the free body diagrams that we will use to explain the static representation of the pulley-type heat engine. Here we are assuming that the pulleys are not turning, hence the model is static.

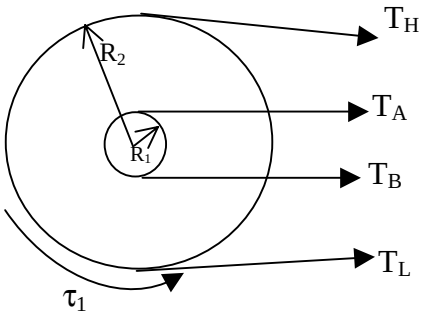

Figure 5.2a: Free body diagram of pulley 1.

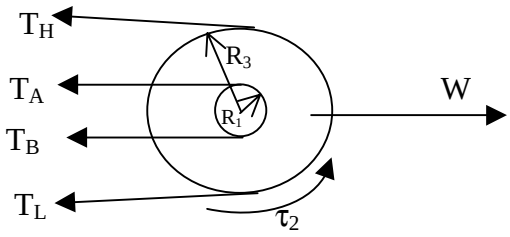

Figure 5.2b: Free body diagram of pulley 2.

Where,

T_H = chain tension in high temperature conditions (above the transition temperature)

T_L = chain tension in low temperature conditions (below the transition temperature)

T_A = synchronizer chain tension on the hot side of the SMA chain

T_B = synchronizer chain tension on the cold side of the SMA chain

τ_1 = resistive torque on pulley 1

τ_2 = resistive torque on pulley 2

Notice that the difference in tension between the top and the bottom cables is a direct result of the difference in temperature. Taking moments in the clockwise direction, we get the following equations for each body:

$$\sum M = 0 \qquad \textit{Equation (5.1)}$$

Thus for body 1:

$$(T_H - T_L)\, R_2 + (T_A - T_B)\, R_1 = \tau_1 \qquad \textit{Equation (5.2)}$$

And, for body 2:

$(T_L - T_H) R_3 + (T_B - T_A) R_1 = \tau_2$ *Equation (5.3)*

Use the following simplifications:

$\Delta R = R_2 - R_3$ *Equation (5.3)*

$\Delta T = T_H - T_L$ *Equation (5.4)*

Rewriting equations 5.2 and 5.3, and summing them together gives:

$\Delta T\ R_2 - \Delta T\ R_3 + (T_A - T_B) R_1 - (T_A - T_B) R_1 = \tau_1 + \tau_2$ *Equation (5.5)*

Thus,

$\Delta T\ R_2 - \Delta T\ R_3 = \tau_1 + \tau_2 = \tau_{res}$ *Equation (5.6)*

Simplifying the equation further:

$(R_2 - R_3)\ \Delta T = \tau_{res}$ *Equation (5.7)*

$\tau_{res} = \Delta R\ \Delta T$ *Equation (5.8)*

Therefore, we can say that there is a resultant torque generated for the configuration shown in Figure 5.1, since both ΔR and ΔT are greater than zero. We also know that the resultant net torque is positive, because both ΔR and ΔT are positive. Since we have assumed a static model, the shafts of the two pulleys are fixed and no motion can occur. It is clear, however, that the resultant torque on the left-hand pulley is in the opposite direction of the resultant torque on the right-hand pulley. Without the synchronizer chain, the two pulleys would rotate in the opposite directions until the difference in belt tension was eliminated. The synchronizer ensures that the pulleys rotate in unison, which ensures a net motion of the system. We will expand the above model to the dynamic case in the following section.

Dynamic Model

Unlike the static case, described above, we will assume that the two pulleys are going to turn in one direction. Consider figure 5.3 below:

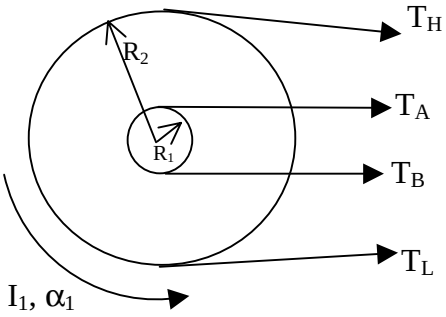

Figure 5.3a: Free body diagram of pulley-1.

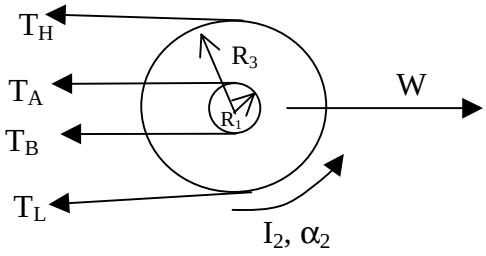

Figure 5.3b: Free body diagram of pulley-2.

Where:

α_1, α_2 = angular acceleration of body-1, and body-2 respectively

I_1, I_2 = mass moment of inertia of body body-1 and body-2 respectively

The equations are similar to the static case,

$$\sum M = I\alpha \qquad \textit{Equation (5.9)}$$

Thus for body-1:

$$(T_H - T_L)\, R_2 + (T_A - T_B)\, R_1 = I_1\alpha_1 \qquad \textit{Equation (5.10)}$$

And, for body-2:

$$(T_L - T_H)\, R_3 + (T_B - T_A)\, R_1 = I_2\alpha_2 \qquad \textit{Equation (5.11)}$$

Rewriting equations 5.10 and 5.11, and summing them:

$$\Delta R\, \Delta T = I_1\alpha_1 + I_2\alpha_2 \qquad \textit{Equation (5.12)}$$

Since the chains are synchronized, the alphas should be equal

$\alpha_1 = \alpha_2 = \alpha$ *Equation (5.13)*

Thus,

$\Delta R\, \Delta T = (I_1 + I_2)\alpha$ *Equation (5.14)*

$\Delta R\, \Delta T = (I_1 + I_2)\, \alpha$ *Equation (5.15)*

Therefore,

$$\alpha = \frac{\Delta R \Delta T}{(I_1 + I_2)}$$ *Equation (5.16)*

Equation 5.16 shows that there is going to be motion in the direction indicated, since the value of the angular acceleration is non zero. From the static and dynamic modeling, we can conclude that the system has the ability to convert heat energy to mechanical work. Johnson's heat engine, described in Chapter 3, is a proof that such a system can work. However, Johnson's heat engine has inherent slip and uses gears to synchronize the system. The VT1 heat engine attempts to eliminate slip by replacing the pulleys by sprockets, the SMA wire by SMA chain, and the synchronizing gears by a chain.

Like most inventions, the final VT1 engine design came about after several changes and improvements. In the following section, I will describe the different stages of the design process. Our first attempt was a design without a synchronizer.

Design I: The engine without a synchronizer

Johnson's engine used a gear type synchronizer, but it wasn't clear at first why this component was essential. The static model seemed to suggest that the engine would produce net torque without the synchronizer so we left it off on our first prototype. We observed small rotations of the sprockets that were in opposite directions. It then became clear that we could not simply add the torque from the two free body diagrams together to get a net torque output, because the two pulleys had no kinematic coupling. , We then

realized the need to couple the motions, hence Design II, an engine with a timing belt synchronizer.

Design II: An engine with a timing belt synchronizer

In order to force the two sprockets to turn in the same direction, we coupled their motion using a timing belt. This belt would engage toothed pulleys mounted on the same axes as the sprockets. Further, the gears were attached to the sprockets so that both the sprocket and the synchronizing gear would turn together.

Before we could apply the heat source, we noticed that there was one problem with this design. The belt kept jumping tooth when we tried to turn it by hand. We assumed that the belt was not strong enough so we changed the synchronizing belt to a roller chain and the gears with a sprocket.

Design III: An engine with a roller chain synchronizer

The third stage of the design process involved implementing a stronger synchronizer to Design II. The synchronizer consists of a roller chain and two sprockets with the same number of teeth; both made from steel. The purpose of the synchronizer, as mentioned earlier, is to force the two plastic sprockets to turn at the same speed (synchronize them). Without the synchronizer, the system will have problems explained below.

Figure 5.1 shows two sprockets, represented as circles and SMA chain lengths a, b, and c.

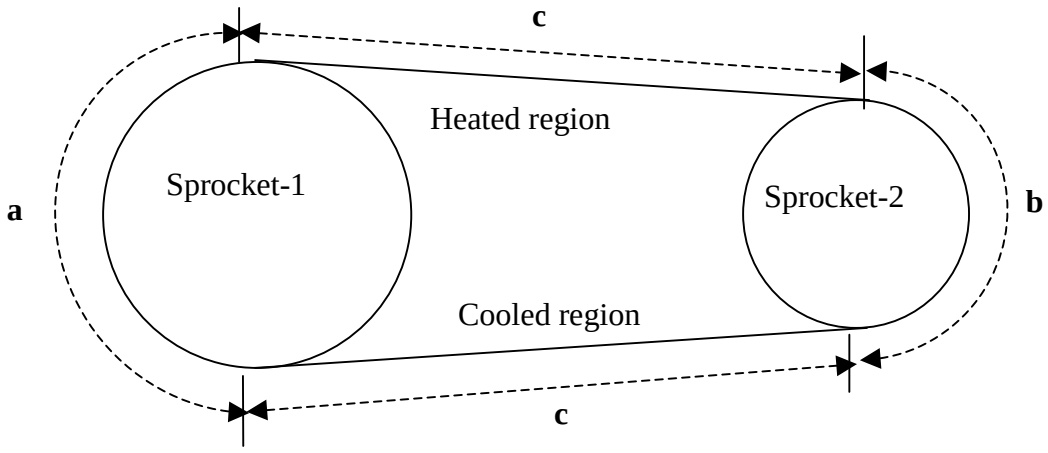

Figure 5.4: Sprocket-1 sweeps more material than sprocket-2, stretching the chain in the cooled region and damping more material in heated region.

Since the sprockets have different diameters, they carry a different length of material at any given time. In a given time span, sprocket 1 carries a length A of material into the heated region, while sprocket 2 carries a length B into the cooled region. Since A is larger than B, more material will be moved into the heated region while more is demanded from the cooled region, assuming clockwise rotations. The system can accommodate the demands, because the heated region of the SMA-chain shrinks absorbing the excess material, and the cooled region stretches, because SMAs can stretch easy when cold. Unfortunately, our initial design used sprockets with equal pitch. Since the chain is a continuum, this forced the rollers to engage and disengage each sprocket at the same rate. Because the chain material between each roller is fixed, this design did not allow the system to move more material into the heated region than was being demanded from the cooling region.

Sprocket-1 has more teeth on it; 24, compared to sprocket-2 that has 23. The sprockets engage with the chain at discreet points. The synchronizer forces the sprockets to turn at the same speed; i.e. both sprockets should pick the same number of teeth. Since the sprocket have different number of turns, just before completing a cycle, there will be one more chain roller picked up by sprocket-1 that can not be accounted by sprocket-2.

If sprocket-1 sweeps five rollers at a time, then sprocket-2 should do the same for them to turn at the same speed. The sprockets may sweep equal number of rollers for less than a cycle, but just before sprocket-2 completes a cycle, sprocket-1 will have to jump a tooth since it is being forced to move at the same speed as sprocket-2. Mathematically speaking:

Given N_1, N_2, N_3, and N_4 to be the number of teeth on sprocket 1,2,3, and 4, respectively (Figure 5.9). Let ω_1, ω_2, ω_3, and ω_4 be the corresponding angular speeds.

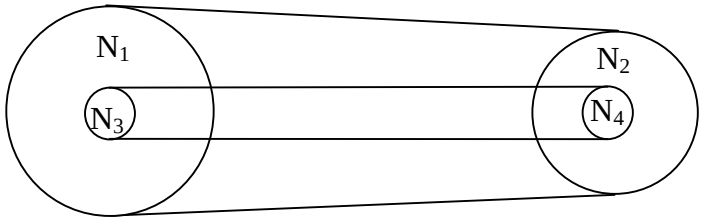

Figure 5.9: Sketch showing four sprockets with teeth numbers N_1, N_2, N_3, and N_4.

From our knowledge of gear trains we know that

$$\frac{N_1}{N_2} = \frac{\omega_2}{\omega_1} \qquad \textit{Equation (5.29)}$$

Thus,

$$\frac{N_1}{N_2} = \frac{N_3}{N_4} = \frac{\omega_2}{\omega_1} = \frac{\omega_4}{\omega_3} \qquad \textit{Equation (5.30)}$$

But, because of the boundary condition imposed by the synchronizer chain, the angular velocities have to be equal. That is,

$\omega_1 = \omega_2 = \omega_3 = \omega_4$ *Equation (5.31)*

Thus, for equation 5.30 to be true,

$N_1 = N_2 = N_3 = N_4$ *Equation (5.32)*

This is contradictory to what we have designed, showing that you cannot drive two sprockets at the same speed and expect them to have different number of teeth. These observations seem obvious in hindsight, and they lead to our next design.

Design IV: Sprockets with Different Pitch, but with the Same Number of Teeth

In this design, one of the sprockets is changed. The sprockets are made to have the same number of teeth, but different pitch. Sprocket-1 has a pitch length of 0.78in and sprocket-2 has a pitch length of 0.75. Hence, sprocket-1 is larger than sprocket-2. When the top portion of the chain is heated, the chain contracts reducing the chain pitch. The chain engages with sprocket-2 with ease, because it has a reduced pitch that is equal to the chain pitch. When the chain reaches the cool region, it will be stretched for the same reason that we explained in the previous designs. That is, sprocket-1 demands more material from the cool region, since it is larger in diameter. Sprocket-2 is smaller than sprocket-1, therefore it can not supply the demand adequately unless it moves faster. Since it has the same speed as sprocket-1 (the synchronizer enforces equal speed), the chain that is in the cool region has to be stretched to a pitch length that is equal to the pitch length of sprocket-1.

In our earlier prototypes, we failed to understand the need for the two sprockets to have different pitches. In hindsight, this seems obvious, and it also points out the important improvement this design offers compared to Johnson's design. While this may at first appear to be a complication in the overall design, we believe the concept of unequal fixed pitch represents an important improvement in the design of band-type SMA heat engines. The fixed pitch of the sprockets holds the chain links at the proper spacing until they enter the free spans where heating or cooling occurs. Earlier designs, such as the one patented by Johnson, depend on friction to prevent belt elongation or contraction while the belt is on the pulley. This obviously leads to some slipping in the

regions near the free spans. If the slipping progresses around the pulley to the other free span, the synchronizer is no longer effective, and the device will cease to operate. Any slipping that occurs decreases the efficiency of the device, because all the work associated with this motion is lost to frictional heating.

The next question would be "what should be the pitch difference between the sprockets so that we can achieve a strain that is within the limits suggested by manufacturers, 4 to 5%?" The limit of stretch comes from the ratio of the sprockets diameter/pitch, as explained in Chapter 4. Stretching above the elastic limit of the chain will damage the chain. Manufactures suggest that the strain should be limited to about 4 to 5%. The difference in pitch limits the strain in the chains. A 0.78in and a 0.75in pitch were chosen to satisfy this condition. Equation 5.33 shows this,

$$\text{Strain} = \frac{\text{final length - initial length}}{\text{initial length}} = \frac{0.78-0.75}{0.75} = 0.4 = 4\% \qquad \textit{Equation (5.33)}$$

Similarly, the difference in diameter of the sprockets shows the 4% limit on the strain.

For sprocket-1,

Number of teeth, N = 23

Pitch, $P_1 = 0.78$

Diameter, $D_1 = P_1N/\pi = 0.78 * 23/\pi = 5.71$in

$D_2 = P_2N/\pi = 0.75 * 23/\pi = 5.49$in

Therefore, strain=5.71-5.49/5.49 = 0.4 = 4%

In summary, not all the parts that go into the VT1 heat engine are presented in this chapter. I described only those parts that I felt needed more explanation. All other parts are presented in Appendix B.

Chapter 6

Thermodynamic Modeling of the VT1 SMA Heat Engine

Introduction

There are two significant works that relate to the thermodynamic aspect of SMAs. The first is by Dr. Johnson, who invented one of the heat engines we looked at in chapter 2. The other work, which will be briefly considered, is the work by Cory, a prominent scientist and founder of Cory Laboratories.

Both works were presented in the same year, 1978. We will start out with Dr. Johnson's work. He approaches the idea of SMA heat engines from the concept of liquid-gas heat engines first, and then creates an analogy between it and SMA engine. The goal is to develop a thermodynamic model that can be used to calculate engine efficiency. Although we might consider efficiency unimportant when dealing with waste heat, as we are claiming is the source of heat in SMA engines, it is a good measure of how well we can improve the performance of the engine. The model will help us determine what part of the cycle is most important. It may also help us diagnose any trouble while operating it. We will first look at a Carnot cycle as it applies to liquid-gas system.

Carnot Engine for a Liquid-Gas System

The Carnot engine is the standard of performance of all heat engines operating between a high and a low temperature. The Carnot efficiency is the limiting case for any engine. Such an engine converts heat energy to work with the maximum efficiency possible. In order to understand the operation of a Carnot engine, we will use an illustrative system as shown in Figure 6.1.

The engine operates while exchanging heat with two energy reservoirs. There are four processes involved: two reversible isothermal processes and two reversible adiabatic processes (Jones, 293). The word adiabatic means "without heat transfer" and the word isothermal means "same temperature." Please, note that this is an ideal case; no system has ever performed to the standard of Carnot efficiency, but it is a good measure of limiting efficiency.

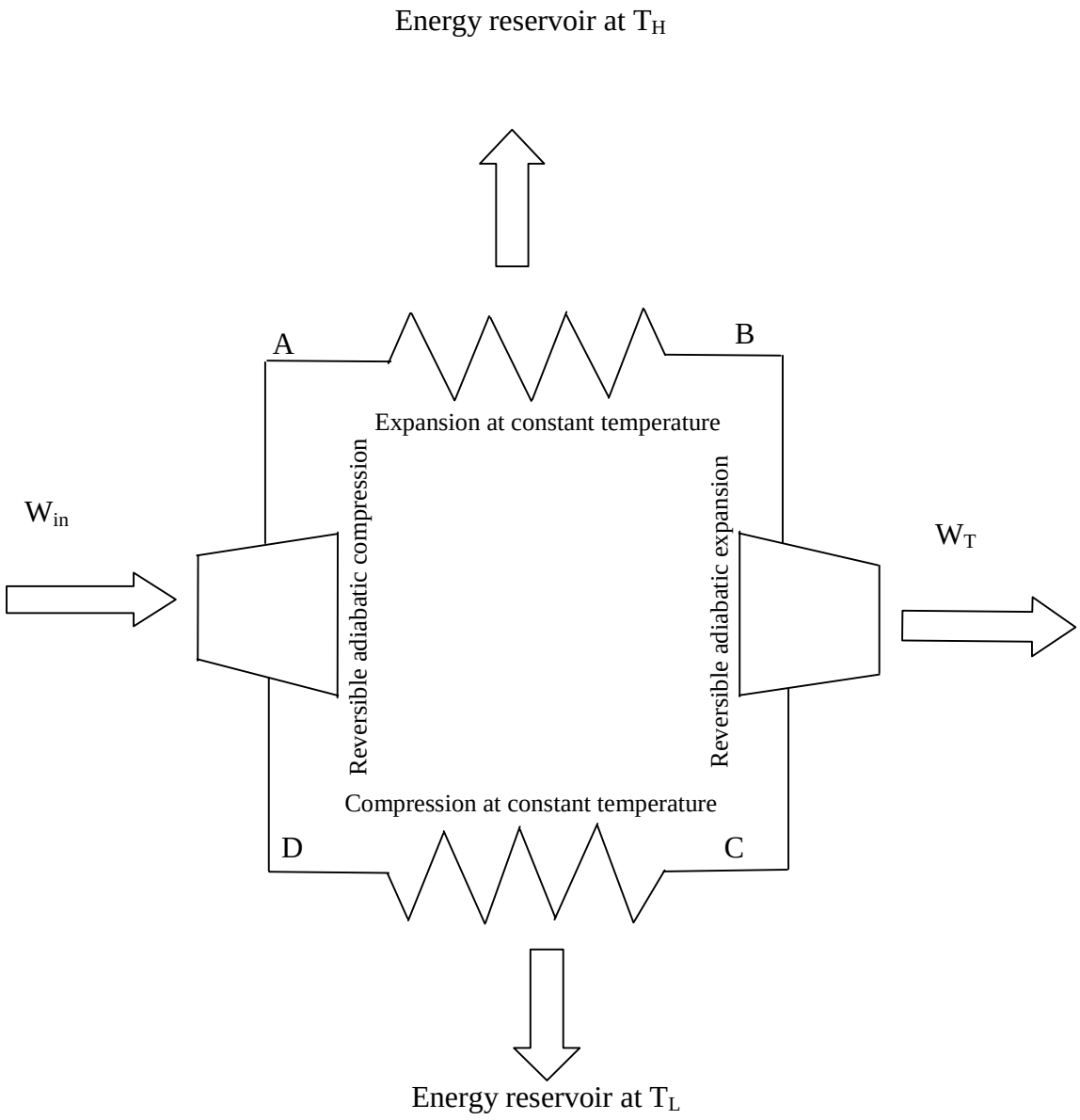

Figure 6.1: Steady-flow Carnot engine using a liquid-vapor mixture as working substance [Jones, 295]

The four cycles that the working substance undergoes are expansion by heating at a constant high temperature; reversible adiabatic expansion; compression by cooling at a constant low temperature; and reversible adiabatic compression. The engine receives heat from a heat source during the expansion at high temperature, it delivers work during the reversible adiabatic expansion, it rejects heat to the heat sink during the compression at low temperature, and, finally, it receives work during the reversible adiabatic compression. The graphical representation of the above system is shown on Figure 6.2.

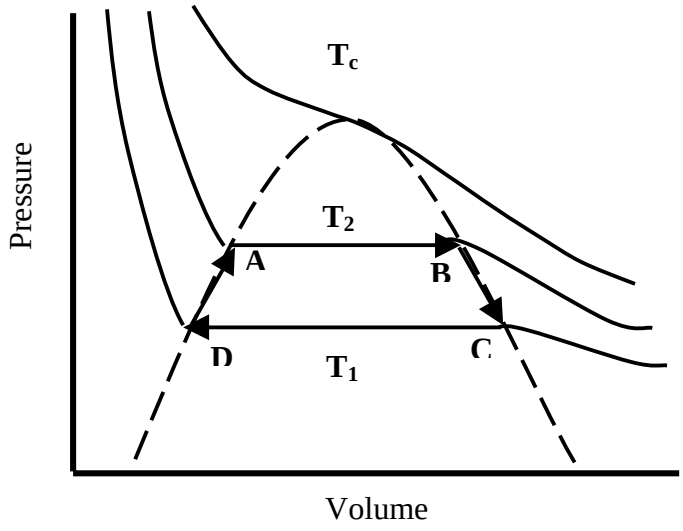

Figure 6.2: Sketch of Pressure-volume relationship of a liquid-gas system [IECEC, 1975, 531].

T_c is the temperature above which the two phases, liquid and gas, are indistinguishable. Below it, isotherms develop plateaus. The dotted line, generally referred to as the dome, joins the start and finish of the plateaus. Within the dome, the liquid and the gaseous phase co-exist in equilibrium. The path ABCDA represents a simple heat engine cycle.

The working fluid in the liquid phase boils at T_2 (line AB) and the expansion of gas does work at constant pressure on the surroundings given by

$$\int PdV \qquad \textit{Equilibrium (6.1)}$$

During the expansion process, a high temperature reservoir supplies heat to the system in order to maintain a constant temperature, T_2. As the gas expands, its temperature tends to decrease, therefore, there is continues supply of heat to maintain the temperature constant along the expansion path A-B. During this first stage, the working fluid undergoes a phase transformation, liquid to gas.

The gas expands further, doing work adiabatically (no heat transfer). Consequently, its temperature drops from T_2 to T_1 along line BC. Gas turbines operate between point B and C (figure 6.1), as the gas expands adiabatically. Once the kinetic energy of the gas is used-up, it then compresses isothermally along line CD; a low-temperature reservoir keeps the temperature at T_1. At this stage of the cycle, another phase transformation occurs. The working fluid transforms from the gaseous state to the liquid state. Finally, the gas compresses adiabatically to the initial state, and its temperature increases from T_1 back to T_2. Note that the area within the PV diagram represents the net work of the reversible liquid-gas cycle. From conservation of energy and the second law of thermodynamics, the maximum thermal efficiency of a heat engine is given by (Johnson, 530):

$$\varepsilon_{\max} = \frac{\Delta W_{\max}}{\Delta Q_{\max}} = \frac{T_1 - T_2}{T_1} \qquad \textit{Equation (6.2)}$$

Where T_1 is the temperature of the cold reservoir and T_2 is the temperature of the hot reservoir, in degrees Kelvin. And ΔW and ΔQ are the net work output of a cycle and gross heat added, respectively. Dr. Johnson proposes that the above relationship can be

used to calculate the theoretical efficiency of SMA heat engines using a stress-strain relationship, Figure 6.3.

SMA Heat Engine Limitation

In SMA engines, the phase transformation occurs between two forms of the solid phase, namely martensite and austenite. All the deformation that takes place occurs with little energy loss by migration of twinning boundaries within individual crystals. Twinning is a reversible process, because no atomic bonds are involved. It is a process where groups of atoms align themselves in a certain preferred orientation (Chapter 2 presents the twinning process). This phase transformation is similar to the phase transformation that occurs in liquid-gas mixtures, because both systems involve phase transformation that resulted from temperature changes. A phase plot, similar to the liquid-gas phase diagram, shown below, shows the analogy between the two systems more clearly.

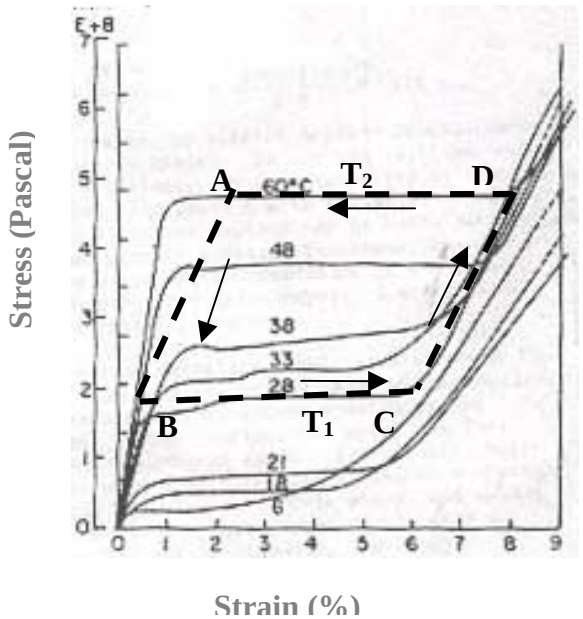

Figure 6.3: Plot of stress- strain relationship for a 0.5mm nitinol wire held at a series of fixed temperatures.

The above figure shows the stress-strain relationship generated from a test conducted on 0.5mm diameter nitinol wire. Each isotherm has a plateau, similar to the liquid-gas system, at which the wire yields plastically until it reaches an elongation, which may be as high as 8% depending on the temperature, and then resumes a normal stress-strain behavior. Wires used in nitinol heat-engines deform along one of the isotherms, and contract along another isotherm. The inverted dome, similar to that of the liquid-gas phase, marks the start and finish of the two phases of SMAs, the martensite and the austenite phase. The rectangular outline, on the stress-strain diagram of nitinol, represents a possible nitinol Carnot heat engine cycle, analogous to that in figure 6.2 for a liquid-gas cycle (Johnson, 531).

Dr. Johnson uses this idea of Carnot cycle to present the limitation on a given nitinol engine that operates between a high and a low temperature. The analogy will help us determine how much we can improve the VT1 heat engine. Liquid and gas were the

working fluids in the Carnot cyclic system. The SMA chain is the working material for our case. This material undergoes phase transformations just like the liquid-gas system.

Assuming that the engine operates between the boiling point of water and room temperature, as is the case for the VT1 engine, we can approximate the efficiency of the engine as proposed by Dr. Johnson. Assume that $T_1 = 100^oC$, and $T_2 = 27^oC$. Theoretically, a nitinol engine using hot and cold reservoirs near boiling and freezing temperatures has a Carnot efficiency near 20% compared to gas turbines whose efficiencies have reached 35% (Spakovsky, 101).

$$\varepsilon_c = \frac{T_1 - T_2}{T_1} \approx \frac{373 - 300}{373} = 0.20 \qquad \textit{Equation (6.3)}$$

Given the above conditions, the VT1 heat engine can not perform better than a 20% efficiency. The amount of energy that we can get out of such reversible cycle is limited to the given efficiency.

Dr. Johnson proposes a second method of calculating efficiency for such heat engines by using the method of entropy. Entropy is property of a thermodynamic system whose change in any differential reversible process is equal to the heat absorbed by the system from its surroundings divided by the absolute temperature of the system. It is independent of any thermodynamic path taken. Figure 6.5 shows a sketch of temperature verses entropy, as presented by Dr. Johnson.

The points A, B, C and D, on fig. 6.5 represent some point in the cycle of the engine. I will propose possible locations for these points on the VT1 heat engine.

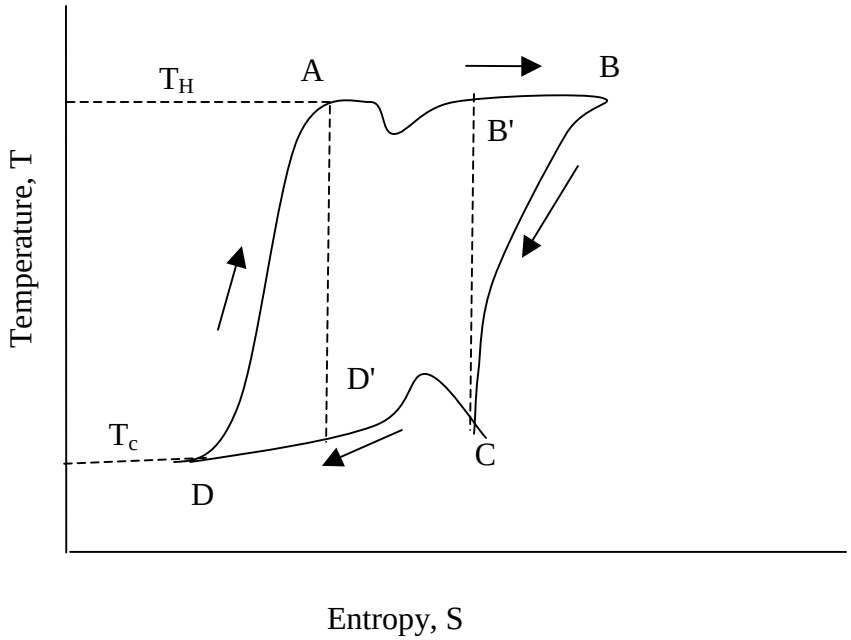

Figure 6.4: Theoretical plot of temperature versus entropy of a heat Engine [Johnson, 533].

From the definition of entropy,

$$\Delta S = \int \frac{dQ}{T} \qquad \textit{Equation (6.4)}$$

it is possible to calculate ΔS for any segment of path along which T is constant and for which ΔQ is measured.

Assume that the distance BB' and DD' are made to approach zero. Then the amount of energy available to do work is ΔQ_{AB} minus ΔQ_{CD} while the total heat input is ΔQ_{AB}. But,

$$\Delta Q_{AB} = \int_{A}^{B} T dS = T_H \Delta S \qquad \textit{Equation (6.5)}$$

$$\Delta Q_{AB} = \int_{C}^{D} T dS = T_C \Delta S \qquad \textit{Equation (6.6)}$$

So maximum efficiency (Carnot efficiency), ε_{max}, is

$$\frac{\Delta Q_{AB} - \Delta Q_{CD}}{\Delta Q_{AB}} = \frac{T_H \Delta S - T_C \Delta S}{T_H \Delta S} \qquad \textit{Equation (6.7)}$$

Dr. Johnson further goes to say that if we take BB' and DD' into account, we may calculate a better approximate of efficiency.

$$\varepsilon_{max} = \frac{\text{energy available to do work}}{\text{heat energy input}} \qquad \textit{Equation (6.8)}$$

$$= \frac{\left(\int_{A}^{B} T_H dS - \int_{B}^{B'} T_H dS\right) - \left(\int_{C}^{D} T_C dS - \int_{D}^{D'} T_C dS\right)}{\left(\int_{A}^{B} T_H dS - \int_{B}^{B'} T_H dS\right)} \qquad \textit{Equation (6.9)}$$

$$= \frac{\left(\Delta Q_{AB} - \Delta Q_{BB'} - \Delta Q_{CD} - \Delta Q_{DD'}\right)}{\Delta Q_{AB} - \Delta Q_{BB'}} \qquad \textit{Equation (6.10)}$$

"Note that it is necessary to measure the above ΔQ's in order to estimate an efficiency. This has never been done systematically. Using crude data which are available (and a somewhat more complicated arguments) Oleh Weres has estiated that such an engine may achieve up to 80% of Carnot efficiency [Weres, 1964]" (Johnson, 534).

Points A, B, C, and D from the cycle occur at the corresponding points shown in figure 6.3 and figure 6.4. Although there are no discrete components, such as compressors and turbines in the case of our VT1 system, we notice that there are four distinct regions. Regions we can relate to in terms of thermodynamic cycle, figure 6.5

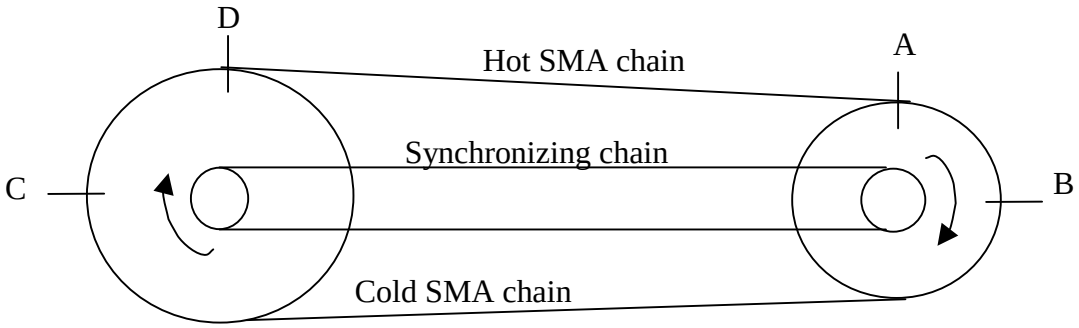

Figure 6.5: Sketch of the VT1 Nitinol Heat Engine

The first region is Region D-A. Here is the area where the SMA chain undergoes transformation from martensite to austenite phase. The chain contracts as heat is added to the system. It is here that the chain experiences maximum tension. The lowest tension region is between B and C, where the chain is immersed in cooling fluid. The model assumes that points C and D are at the same temperature, that is, the path CD is on an isotherm. Similarly A and B are on the same isothermal line. We can argue that the model is an exaggeration of what is really happening with the VT1 engine, but it is similar to the use of a Carnot engine to find the ideal efficiency.

Cory did the second type thermodynamic analysis on SMA heat engines (Cory, 1978). He proposes three models using state relations force, length, and temperature (FLT). The first model he presents is a TA- cycle, an isotherm-adiabatic cycle. The second model is a TL-cycle, isothermal-constant length cycle. And, the last is the FL-cycle, constant force-constant length cycle. It is hard to model the VT-1 heat engine as one of these three models, because it seems that the engine is a combination of the models. Therefore, I will not pursue investigating Cory's model any further. It will be up to the discretion of the reader to investigate these thermodynamic state models.

Limitations on the Performance of the Engine

There are two major limitations on the performance of the engine; namely, the rate of heat transfer, and the rate of phase transformation. The rate of flow of heat will dictate how fast the engine will be running. If enough heat is supplied to the heated region of the engine, it undergoes phase transformation and induces motion. However, if it is not cooled when it gets to the region where it is supposed to be cooled, no more motion can be extracted from the system, because it cannot revert its transformation. Heating it in one region and cooling it in another will insure continuity of the motion. How fast we heat it and how fast we cool it will dictate how fast it is going to run. The rate of heating and cooling need to be equal for it to run at an optimized speed.

The other limitation on the performance of the engine is its ability to transform its phase. Even if we are able to heat the chain instantly and cool it just as fast, unless the phase transformation occurs faster than the rate of heating and cooling, we will not be able to run the engine any faster. Normally, phase transformation time is very small; fractions of a second. But, it does set a boundary on how fast the engine can run. Conducting some measurements to determine this limitations is essential.

It is hard to measure the rate of heat flow, because such measurements would require a highly controlled environment. For example, any water droplet carried by the

chain when moving from the cooled region to the heated area will complicate temperature measurement, since mixing will occur between the hot and cold baths. Therefore, we do not recommend using Equation 6.10 to calculate at this point of the design stage. But, efficiency can be approximated using Equation 6.3 with relative ease. Equation 6.3 requires only temperature measurements. Assuming steady state conditions, we can measure the temperature of the chain using the method of Infrared temperature measurement.

Another important parameter that is essential in characterizing the VT1 is the power that it produces. The power of an engine is the rate at which the engine does work. It determines the possible application of the engine. One of the methods to measure power is by using a dynamometer. This instrument can also measure speed, which is another important parameter. Plot of power verses speed is commonly used in characterizing engines.

Chapter 7

Conclusions and Recommendations

The purpose of this thesis work was to present the design and analysis of an improved heat engine made using shape memory alloy. In light of the past work that has been attempted in this area, it seems unlikely that the earlier inventions could be scaled up to the point where they have practical utility. This thesis presents a new design that has the potential to be the basis for large SMA engines.

The first part of the work presented a review of some of the theoretical background on SMAs. We saw that SMAs are materials that "memorize" their shape at specific temperatures. At low temperatures, they are easy to deform, but at increased temperatures they exert large forces as they try to recover their original shape. This reversible property is attributed to their unique solid phase transformation known as martensitic transformation.

The large force and displacement that results from the phase transformation raised interest in the area of heat engines. The first heat engine was built by Ridgway M. Banks in 1973. The engine turned 70 rpm and produced about half a watt of power. Other engines were built afterwards, but non of these was reported to have had any success in scale up models.

The engine that is most similar to the VT1 engine was invented by Dr. Johnson, in 1976. His design used pulleys and helical coils that were synchronized using gears. The

engine operated for several thousand cycles, but there was no success in scaling it up because of frictional and slip loses associated with the design.

The VT1 engine is an improvement on the Johnson's design. It implements a chain/sprocket drive system and a chain/sprocket type synchronizer. We believe that the VT1 has the potential for scale up, because it uses a mechanism that can allow it to transmit large torque, and it eliminates large friction losses associated with previous designs.

While this thesis lays the groundwork for developing this new device, many question remain to be answered. The final design is still under construction, but the work presented in this thesis provides evidence that the engine will work. Still, the first functional prototype of the VT1 engine remains to be demonstrated. As described previously, the final concept requires a non-standard sprocket with a pitch of 0.78in. While the fabrication of such a sprocket is relatively simple, it is not an off-the-shelf component. The next step in the development is clearly to fabricate this sprocket and then demonstrate the prototype. This is the first major hurdle. Once the device is working, questions regarding efficiency and scalability can begin to be addressed.

Below are some experiments that might help the understanding of the VT1 SMA heat engine.

1) Develop a relationship between source and sink temperature and speed
2) Vary the length of the chain and see the effect on torque and speed
3) Vary the size of the sprocket and investigate its effect on torque and speed
4) Conduct measurements of temperature and heat transfer rates at various points in the system. Although the measurements will be challenging, this will give information helpful in understanding the efficiency of the device.
5) Calculate efficiencies from the heat transfer measurements
6) Optimize the temperature difference. Extreme temperature differences are a source of irreversibility, because of the large amount of entropy

generated. Therefore, the engines cannot approach the efficiency of an ideal engine, or Carnot efficiency.

In conclusion, I would like to point out some of the advantages of the VT1 SMA heat engine. The engine uses few moving parts, which results in a relatively simple design. The use of a roller chain as the synchronizer make the device easy to scale to any length. Immersing a greater length of the chain in the heating and cooling fluid should increase the running speed. Because SMAs are highly resistive to corrosion, the engines can find application in various environmental conditions. In addition, SMA heat engines can operate over a wide range of temperatures, by selecting a thermal memory material having a suitable critical temperature appropriate to the climatic conditions. The SMA heat engines should operate at much lower noise levels than many other engines. All things said and done, there is still an intriguing future for the VT1 SMA heat engine.

Appendix A

References

Books

Betteridge, Nickel and its alloys, 1984

Binder R.C., Mechanics of the Roller Chain Drive, 1956

Cory, J.S. and McNchols, J.C., Society of Automotive Engineers, Inc., 1978, pages 1998-2004.

Center for Intelligent Materials of Virginia Polytechnic Institute and State University
310 New Engineering Building (Box: 0261)
Virginia Tech, Blacksburg, VA, 24061

Dictionary of Scientific and Technical Terms, McGraw-Hill, 2nd edition

Dye, Tracy Earl, An Experimental Investigation of the Behavior of Nitinol (masters thesis), Virginia Tech, August, 1990

Funakubo, Hiroyasu, Shape memory Alloys, University of Tokyo, 1984

Hodgson, D.E., Using Shape Memory Alloys, Shape memory Applications, Inc., 1988

Johnson A D, IECEC, October 1975, page 530 -534

Jones, J.B and Dugan, R.E., Engineering Thermodynamics 1996, page 186-188

Jackson and Moreland, Design Manual for roller and silent chain drives, 1955

Mabie, Hamilton H. and Reinholtz, Charles F., Mechanisms and Dynamics of Machinery, 1987

Miller, Richard K. and Terri Walker, Survey on shape memory alloys, 1989

Weres, O., The Thermodynamics of Nitinol, Lawrence Berkeley Laboratory internal communication, December, 1964.

Spakovsky, Von M.R. and Olsommer, B., Fuel ell System Modeling and Analysis Perspectives for Fuel Cell Development, ECOS, 1999.

Patents

Banks, Ridgway M., US03913326, Energy Conversion Systems, 1975

Buehler, William J and Goldstein, David. M, US3403238, Conversion of heat energy to mechanical energy, 1968

Dante, Sandoval J., US4030298, Thermal Motor, June 21,1977

Hochstein, Peter A., US3913326, Thermal Energy Converting Assembly, July 26,1977

Horton, Paul F, US4006594, Solar Power Plant, 1977

Johnson A. D., US4055955, Memory alloy heat engine and method of operation, Nov. 1, 1977

Li, Yao Tzu, US4075846, Thermal engine with entrapped working medium, 1978

Warren K. Smith, US4086769, Compound Memory Engine, 1978

Pachter, John J. US4150544, Engine, 1979

Web Pages

LBNL Image Library Collection, Berkeley Laboratories/Research. Global Brain No.157:SPECIAL ENERGY REPORTS: 1) Ridgeway Banks' Nitinol Engine (1973), and 2) Joseph Newman's Energy Machine (Jan 98).
http://www.itg.lbl.gov/ImgLib/COLLECTIONS/BERKELEY-LAB/RESEARCH-1930-1990/MATERIAL-SCIENCES-SOLID-STATE-PHYSICS/index/96904735.html

Weston, David
http://mai.flora.org/forum/1841

A Comprehensive Characteristic Study of NiTi Behavior: Quasi-Static Thermomechanical Loading, Duval, Luis, Soheil Saadat, Mohammad N. Noori, Hamid Davoodi, Zhikun Hou
http://www.formulaconsulting.com/project/clpsi/papers/p0020/paper.html

Shape Memory Applications Inc.
http://www.sma-inc.com/nitivssteel.html

Appendix B

Parts List and Drawings of Parts that were Manufactured in House

Item #	Description	Manufacturer	Mfg. /Order #	Material	Qty.	Price
1	Socket Head Cap Screw, 8-32, 1" Long	McMaster-Carr	92196A199	Stainless Steel	100	$9.52
2	Nut,8-32, 11/32 wide, 1/8 high	McMaster-Carr	90480A009	Zinc Plated Steel	100	$0.91
3	Washer, Size 9, 3/16 ID, 7/16 OD	McMaster-Carr	90126A009	Zinc Plated Steel	100	$4.51
4	Washer, Size 4, 3/16 ID, 5/16 OD	McMaster-Carr	90126A005	Zinc Plated Steel	100	$6.77
5	Roller, 1/2 OD, 1/2 Long, 1/4" Screw Size	McMaster-Carr	94639A142	Nylon	100	$5.37
6	Bolt Spacer, 1/4 OD, 5/8 long, Screw Size 8	McMaster-Carr	92510A307	Aluminum	100	$29.75
7	Bolt Fixture	To Be Mnfd.	-	Steel	1	-
8	Sprocket , 23 teeth, # 60, 0.75" pitch, 1" bore	McMaster-Carr	60425K126	UHMW	1	$31.65
9	Sprocket , 23 teeth, # 60, 0.78" pitch, 1" bore	To Be Mnfd.	-	UHMW	1	-
10	Ball Bearings, 1/2" Shaft Dia.	McMaster-Carr	6244K51	Cast Iron	4	$97.72
11	Sprocket Spacer, 1" OD, 1/2" ID	To Be Mnfd.	-	Aluminum/Brass	2	-
12	Sprocket Shaft, 1/2" OD	To Be Mnfd.	-	Aluminum/Brass	2	-
13	Frame, 20"long x 1 3/16" wide x 1/2" thick	To Be Mnfd.	-	Aluminum	2	-
14	Frame 4 5/8" long * 1 3/16" wide, 1/2" thick	To Be Mnfd.	-	Aluminum	2	-
15	Shaft, 1/2" OD , 10" long	To Be Mnfd.	-	Aluminum	2	-
16	Fluid Container Box, 20"long x 5"high x 5" wide x 1 3/16" thick	To Be Mnfd.	-	Wood/	1	-
17	Roller Indexing Fixture,	To Be Mnfd.	-	Aluminum	1	-
18	Bore Steel Roller Chain Sprockets Number 20, 3/8"Pitch	McMaster-Carr	62375K12	Steel	2	$22.24
19	QD Bushings, Style JA	McMaster-Carr	6086K11	Steel	2	$12.30
20	Steel & Stainless Steel Roller Chain 3/8" Pitch, ANSI NO. 35	McMaster-Carr	6261K531	Steel	1	$2.35
21	Counter Weight	To Be Mnfd.	-	Aluminum	2	-
	Total					**$ 163.91**

Drawings

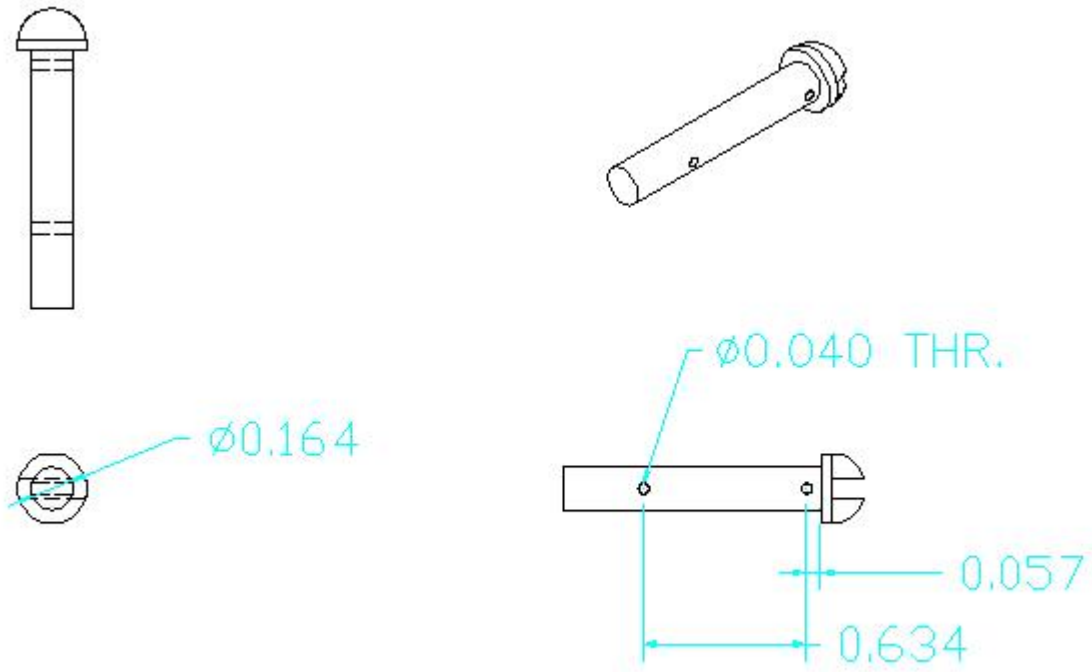

Unless Otherwise Specified,
All Dimensions In Inches
Part Name: **8-32 Bolt**
Material: Aluminum

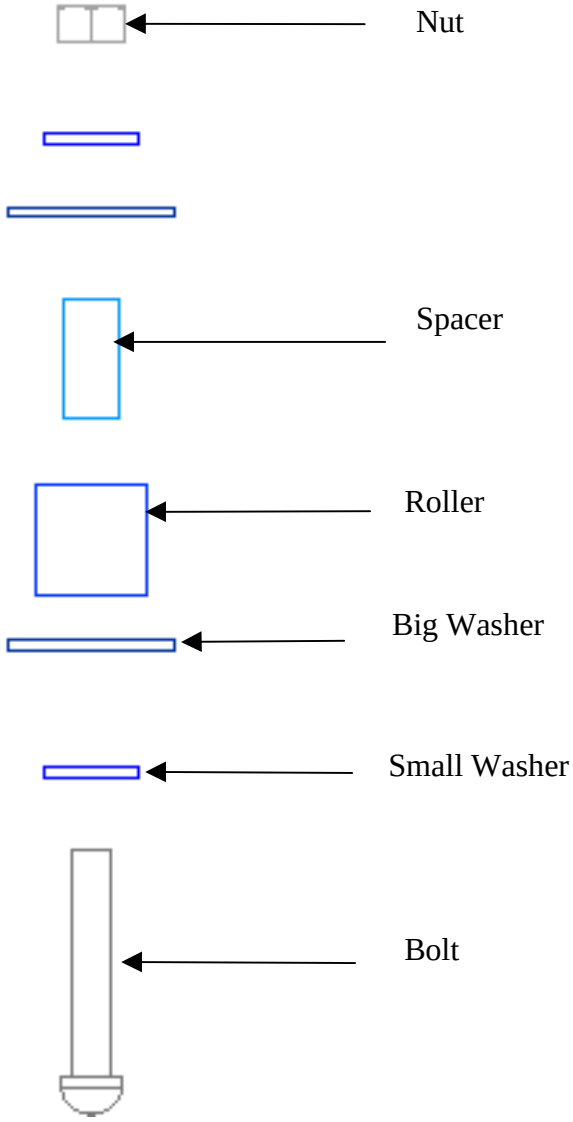

Unless Otherwise Specified,
All Dimensions In Inches
Part Name: **Bolt Assembly Exploded View**
Material: Aluminum

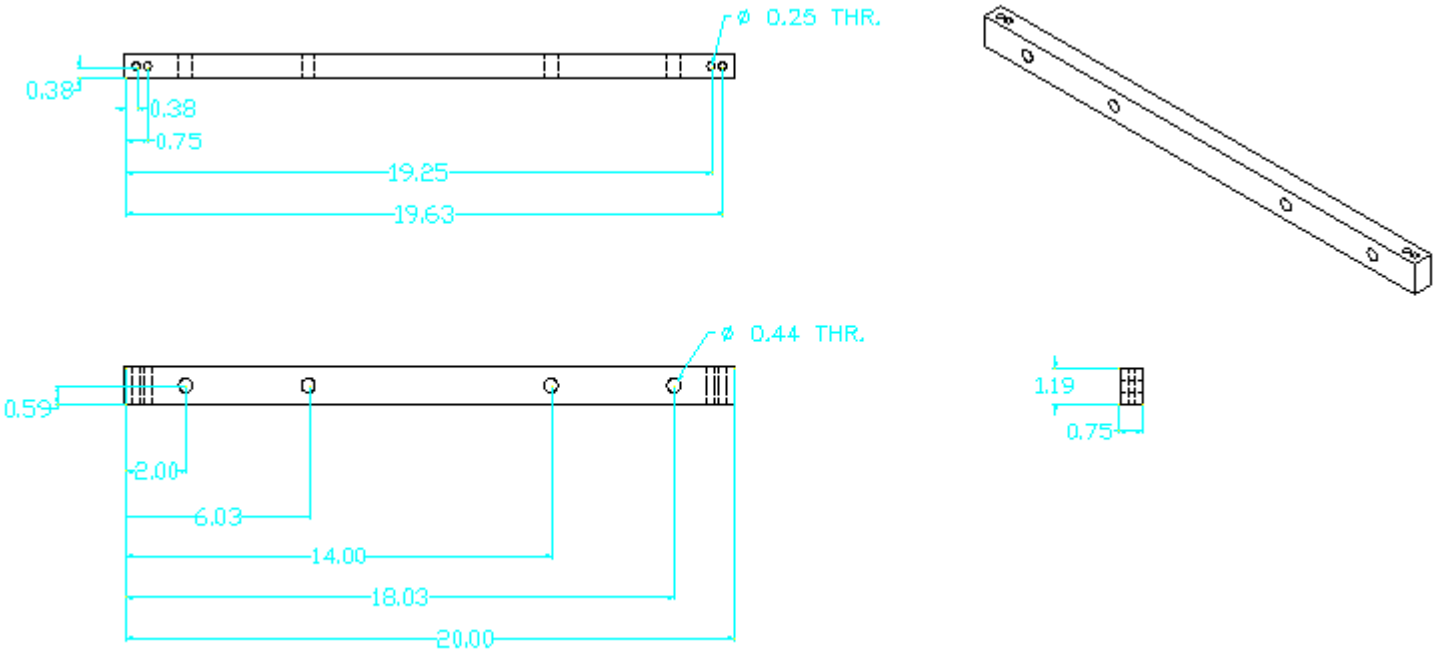

Unless Otherwise Specified,
All Dimensions In Inches
Part Name: **Frame 1**
Material: Aluminum

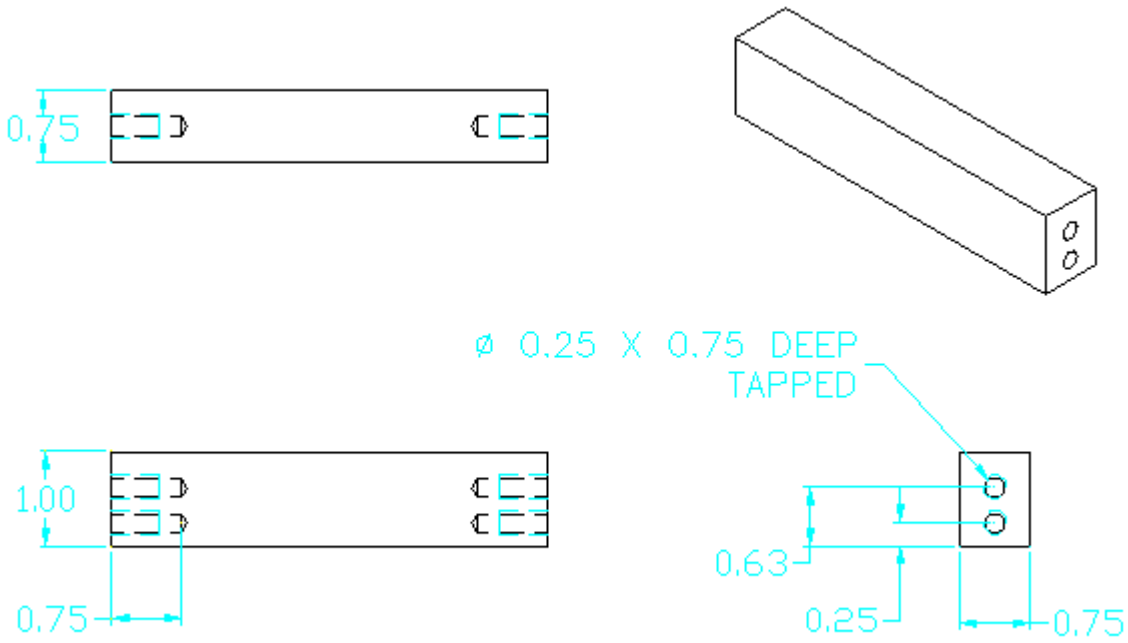

Unless Otherwise Specified,
All Dimensions In Inches
Part Name: **Frame 2**
Material: Aluminum

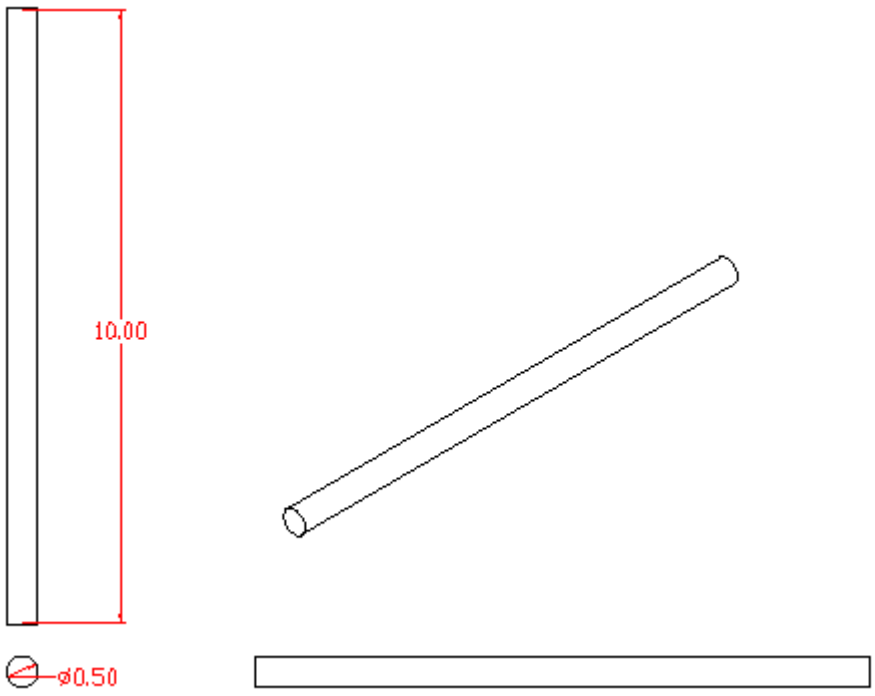

Unless Otherwise Specified,
All Dimensions In Inches
Part Name: **Shaft**
Material: Aluminum

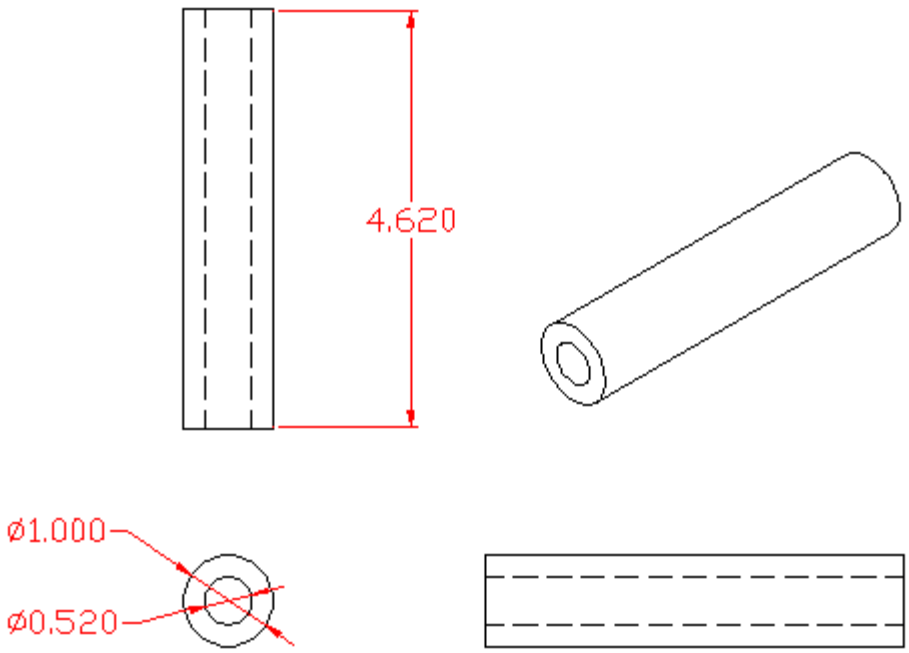

Unless Otherwise Specified,
All Dimensions In Inches
Part Name: **Bearing Spacer**
Material: Aluminum

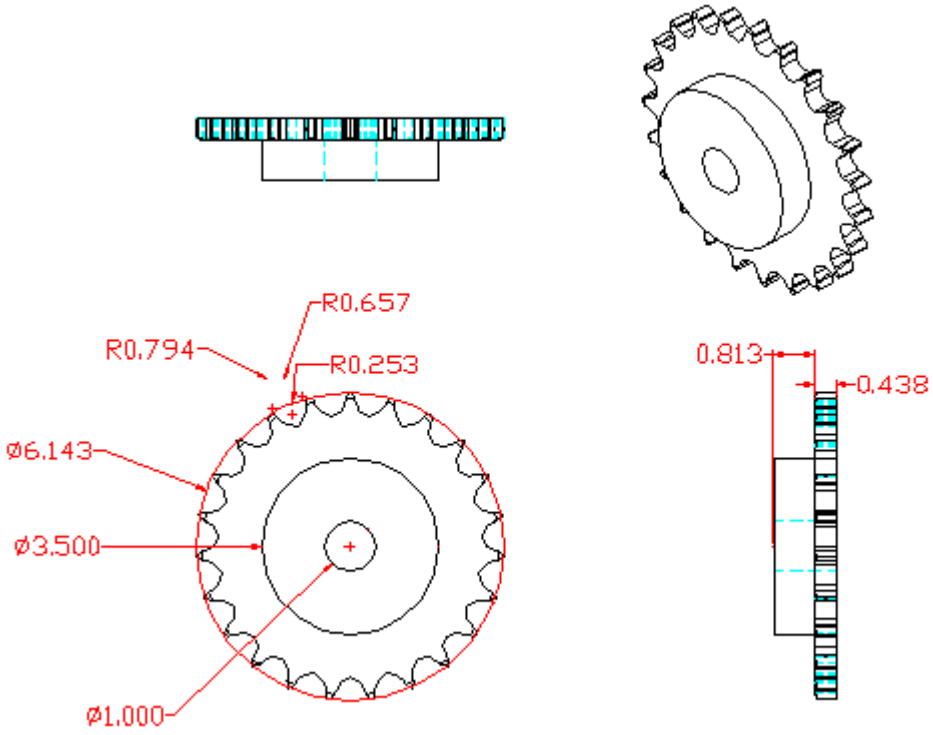

Unless Otherwise Specified,
All Dimensions In Inches
Part Name: **Sketch of a 0.78" Pitch Sprocket**
Material: Aluminum

Vita

Jillcha Fekadu Wakjira was born on August 31, 1974 to Fekadu and Abinet, in Addis Ababa, Ethiopia. He completed his high school study in 1992 at Saint Joseph, while in Ethiopia. Soon he moved to Harare, Zimbabwe and started his Engineering education at the University of Zimbabwe after completing an advanced level study in 1994. While a sophomore at the university, he moved to the US in 1996 and continued his education at Virginia Tech in1997. He graduated with honors in 1999.

Jillcha is currently employed by Corning Cable Systems in Hickory, North Carolina. He plans to get married to Sidissie Tsegaye Bushen on the 30th of June, 2001.